https://doi.org/10.5194/egusphere-2026-235
Preprint. Discussion started: 13 March 2026

Real-time automated quality control of atmospheric aerosol time series

Timo Houben[1,2], Thomas Müller[3], Peter Lünenschloss[1], Jens Voigtländer[3], Thomas Trabert[1,2], Ema Vosgerau[1,2], David Schäfer[1], and Jan Bumberger[1,2,4]

[1]Helmholtz Centre for Environmental Research - UFZ, Research Data Management - RDM, Permoserstraße 15, 04318 Leipzig, Germany
[2]Helmholtz Centre for Environmental Research - UFZ, Department Monitoring and Exploration Technologies, Permoserstraße 15, 04318 Leipzig, Germany
[3]Leibniz Institute for Tropospheric Research (TROPOS), Permoserstraße 15, 04318 Leipzig, Germany
[4]German Centre for Integrative Biodiversity Research (iDiv) Halle-Jena-Leipzig, Puschstraße 4, Leipzig 04103, Germany

Correspondence: Timo Houben (timo.houben@ufz.de)

Abstract. Automated, reproducible quality control (QC) of aerosol optical time series is essential for comparable, reusable data in observation networks and research infrastructures. We present a real-time-capable QC workflow for AE33 Aethalometer equivalent black carbon (eBC) and Aurora 4000 nephelometer scattering measurements (σ_{sca}). The workflow is implemented in the open-source SaQC framework and wrapped by the `actris_qc` package, which encodes community QA/QC recommendations into a three-stage, machine-readable rule set for device-control, channel-specific and derived-variable checks. The pipeline is parameterised using a catalogue of instrument anomalies from the urban TROPOS site and validated at the rural Melpitz station, demonstrating robust transfer across contrasting environments. It reliably flags outliers, noise, plateaus and device malfunctions while preserving genuine atmospheric variability and achieves real-time performance on standard hardware. The modular, configuration-driven design enables straightforward adaptation to additional instruments and networks, providing harmonised QC flags and provenance and enabling FAIR-compliant and AI-ready downstream use in monitoring systems.

1 Introduction

The Earth's atmosphere is a dynamic and highly complex system whose composition and evolution are tightly interwoven with climate, air quality, and ecosystem health. Monitoring and understanding the behaviour of short-lived atmospheric constituents, aerosols, and trace gases is therefore critical to support scientific insight, inform policy, and foster sustainable development. Recognising this need, a suite of coordinated atmosphere-centred environmental research infrastructures (RIs) has been established in Europe, including ACTRIS (Aerosol, Clouds and Trace Gases Research Infrastructure), ICOS (Integrated Carbon Observation System), and IAGOS (In-service Aircraft for a Global Observing System), which together provide harmonised long-term observations of aerosol, trace-gas and greenhouse-gas properties from surface stations and commercial aircraft (Laj et al., 2024; Heiskanen et al., 2022; Petzold et al., 2015). In parallel, terrestrial and ecosystem RIs such as TERENO and eLTER in Europe and NEON in the United States have been developed to observe land–atmosphere exchanges and socio-ecological systems across spatial and temporal scales (Chabbi and Loescher, 2017; Mollenhauer et al., 2018; Zacharias et al., 2024; Ohnemus et al., 2025). These infrastructures are increasingly linked through cluster initiatives (e.g. ENVRI in Europe) and the emerging concept of a Global Ecosystem Research Infrastructure (GERI), with the ambition to provide a distributed, interoperable observing system for the coupled Earth system (Loescher et al., 2022; Petzold et al.,

https://doi.org/10.5194/egusphere-2026-235
Preprint. Discussion started: 13 March 2026

2024).

Across these atmospheric and terrestrial RIs, a common objective is to deliver open, FAIR and analysis-ready data streams that underpin climate services, air-quality assessments, ecological forecasting, and digital decision tools such as Earth system models and digital twins. Recent syntheses on environmental big data and Earth-system digital twins underline that such systems depend on continuously updated, well-characterised and interoperable observation streams (Li et al., 2023; Hazeleger et al., 2024). The environmental data landscape is rapidly becoming data-intensive: multi-parameter, multi-platform observatories generate massive near-real-time data flows that must be quality-assured, traceable, and interoperable in order to be assimilated into advanced AI-based modelling and forecasting systems (Reichstein et al., 2019; Bauer et al., 2021a; Calvin et al., 2023; Petzold et al., 2024). Recent strategic analyses of environmental and ecosystem infrastructures emphasise that their scientific and societal impact critically depends on robust, automated QA/QC and curation workflows that can be applied consistently across instruments, sites, networks and domains – from atmospheric composition to terrestrial ecosystems (Loescher et al., 2022; Petzold et al., 2024). These infrastructures form the empirical foundation for next-generation environmental intelligence systems and digital-twin initiatives envisioned by e.g. the European Green Deal, Destination Earth (DestinE), and AI-enabled Earth-system prediction frameworks (Reichstein et al., 2019; Bauer et al., 2021a, b).

Long-term in situ observations of aerosol particle properties are a cornerstone of both air-quality management and climate research. Filter-based absorption photometers such as the Magee Scientific AE33 Aethalometer and integrating nephelometers such as the Ecotech/ACOEM Aurora 4000 are widely deployed in research infrastructures and regulatory networks to provide black carbon (BC) or equivalent black carbon (eBC) and particle light-scattering coefficients at high temporal resolution (Drinovec et al., 2015; Müller et al., 2011; ACTRIS-2 Consortium, 2018; Asmi et al., 2021). These optical properties are required to quantify the climatic impact of light-absorbing aerosols, to constrain emissions and source apportionment, and to assess human exposure to combustion-related particulate matter.

Most importantly, Directive (EU) 2024/2881 on ambient air quality and cleaner air for Europe has moved black carbon (BC) from a mainly research-oriented metric into the formal European air-quality monitoring architecture. The Directive defines BC as carbonaceous aerosols measured by light absorption and requires fixed BC measurements at monitoring supersites in both urban and rural background environments. At the same time, it explicitly acknowledges that no EN standard method for BC is yet available, which makes current harmonisation and standardisation efforts particularly relevant for cross-site comparability and regulatory uptake (European Parliament and Council of the European Union, 2024).

This regulatory shift is accompanied by recent European guidance and synthesis work on BC and related aerosol metrics, including recommendations on harmonised methodologies, inlet configurations, reporting conventions, MAC selection and the upscale of BC observations to urban and national monitoring applications (Laj et al., 2020; Savadkoohi et al., 2023, 2024; RI-URBANS, 2024; Zheng et al., 2025). These efforts build on the terminology framework proposed by Petzold et al. (2013), recent pan-European recommendations for reporting equivalent black carbon (eBC) and handling MAC variability (Savadkoohi et al., 2024), and the RI-URBANS guidance for BC determinations that was developed specifically in connection with the new Directive (RI-URBANS, 2024). In parallel, the ongoing STANBC metrology project aims to underpin a future CEN standard for traceable BC-related measurements and calibration workflows (European Metrology Network for Pollution Monitoring, 2026).

Within ACTRIS and related initiatives such as RI-URBANS, AE33 and Aurora 4000 instruments have therefore become key workhorses at supersites and urban observatories, where they provide the high-quality reference data needed to evaluate models, support emission abatement strategies and calibrate or benchmark low-cost sensor networks.

Over the past decades, extensive efforts have been invested in developing harmonised measurement protocols and quality-assurance frameworks for such instruments. WMO's Global Atmosphere Watch (GAW) programme and the pan-European ACTRIS research infrastructure synthesise recommended procedures for aerosol in situ measurements, define core variables and data quality objectives, and coordinate intercomparisons and central facilities for calibration and traceability (World Meteorological Organization (WMO), 2016; Laj et al., 2024; ACTRIS CAIS-ECAC, 2026). Similar guidance exists at the regulatory level, for example through the US EPA Quality Assurance Handbook for Air Pollution Measurement Systems and European Commission and JRC documents that describe QA/QC systems and data validation procedures required under the Air Quality Directive European Commission Joint Research Centre (2011); German Environment Agency (2016); U.S. Environmental Protection Agency (2026). For black carbon specifically, recent RI-URBANS and ACTRIS documents summarise harmonised methodologies, correction schemes and reporting conventions for eBC and absorption coefficients, aiming to upscale BC measurements into urban and national networks (Petzold et al., 2013; Laj et al., 2020; Savadkoohi et al., 2023, 2024; RI-URBANS, 2024). However, across these frameworks, the practical implementation of quality control for AE33, Aurora 4000 and related time series remains largely manual: QC typically relies on visual inspection, bespoke scripts

https://doi.org/10.5194/egusphere-2026-235
Preprint. Discussion started: 13 March 2026

and station-specific conventions rather than on a common, automated and reproducible pipeline. This creates a bottleneck for observatories and research infrastructures that increasingly need to deliver analysis-ready data in (near) real time for digital twins, model assimilation and AI applications, and it motivates the development of generic, fully automated QC workflows such as the one proposed in this study.

Despite this mature landscape of QA/QC frameworks, quality control of the resulting time series is still predominantly performed through manual inspection and project-specific scripts. GAW report No. 227, for example, defines quality objectives, recommended instrument checks and general flagging principles, but leaves the implementation of concrete data screening and flagging largely to individual stations and data originators (World Meteorological Organization (WMO), 2016). ACTRIS measurement guidelines for AE33 Aethalometers and Aurora 4000 nephelometers provide detailed instructions on instrument operation and manual quality control, including recommended tests and visual inspection of time series, but again do not prescribe or supply a standardised software pipeline for automated data quality control in near-real-time (Müller and Fiebig, 2020, 2021). US EPA and European QA guidance similarly emphasise management systems, traceability, audits and collocations, while data validation remains a largely manual or semi-manual process performed before archiving and reporting to central databases such as AQS or AirBase (U.S. Environmental Protection Agency, 2026).

At the same time, the technical complexity of aerosol optical measurements makes them particularly vulnerable to systematic errors that accumulate over the lifetime of an instrument. For filter-based absorption photometers, artefacts include non-linear filter loading effects, tape inhomogeneity, and multiple scattering within the filter matrix, which all require empirical correction and can change with filter type and aerosol properties (Yus-Díez et al., 2021; Ferrero et al., 2024). Relative humidity, semi-volatile losses and instrument flow drift affect both absorption and scattering measurements, while inlet and optical fouling, leaks and mis-configurations can introduce subtle but persistent biases that are difficult to detect without systematic analyses. Intercomparison studies and method-focused work for AE33, MAAP and different nephelometers have documented instrument-to-instrument variability, sensitivity to operating conditions, and the need for careful corrections of multiple scattering, angular truncation and illumination effects (Yus-Díez et al., 2021; ACTRIS-2 Consortium, 2017b, 2018). For long-term applications, unrecognised drift, fouling and configuration changes translate into systematic errors in derived eBC mass concentrations and scattering coefficients, with direct consequences for trend analyses, source apportionment, and model evaluation (Laj et al., 2020; Savadkoohi et al., 2024).

These challenges are amplified by the rapid proliferation of additional in situ measurements in environmental observatories and regulatory networks. Advances in dataloggers, telemetry and sensor technology have enabled the deployment of dense networks of both reference-grade instruments and low-cost sensor (LCS) systems, often operating in near-real-time and generating massive data volumes (Okorn and Iraci, 2024; World Meteorological Organization (WMO); United Nations Environment Programme (UNEP); International Global Atmospheric Chemistry project (IGAC), 2024). Scoping reviews of LCS networks and WMO reports consistently highlight concerns about the reliability and fitness-for-purpose of such measurements, and emphasise the need for robust calibration, performance assessment and quality control (World Meteorological Organization, 2021; Carotenuto et al., 2023; Bagkis et al., 2025). However, QA/QC concepts for LCS data are typically developed independently of those for high-end reference instruments and focus on sensor-specific calibration models and co-location strategies rather than on a generic, transferable quality-control pipeline (World Meteorological Organization, 2021; Okorn and Iraci, 2024; Hayward et al., 2024).

Looking ahead, a new generation of applications—urban and regional digital twins, data assimilation in high-resolution air-quality and climate models, machine-learning based forecasting and re-calibration frameworks, and even foundation models for environmental data—are all critically dependent on the availability of long, homogeneous and well-characterised observational data streams. In all of these cases, systematic biases, undetected drifts or unflagged artefacts in the training or assimilation data are very likely to be propagated and amplified by the models, undermining their predictive skill and interpretability. FAIR principles for environmental time series underline that data must not only be findable and interoperable, but also transparently processed and quality-controlled in a reproducible manner (Sheldon, 2008; Campbell et al., 2013; Schmidt et al., 2023; Bumberger et al., 2025).

Manual and semi-manual QA/QC workflows are increasingly unable to meet these demands. They are labour-intensive, scale poorly with network size and temporal resolution, and are prone to subjectivity, as demonstrated by controlled experiments where different experts produced markedly different QC decisions on identical datasets (Campbell et al., 2013; Taylor and Loescher, 2013; Jones et al., 2018). This subjectivity not only threatens reproducibility but also complicates the integration of heterogeneous data streams from distinct networks and initiatives. Moreover, traditional QC frameworks rarely capture the full

https://doi.org/10.5194/egusphere-2026-235
Preprint. Discussion started: 13 March 2026

range of drift, fouling and configuration artefacts that manifest gradually over months to years rather than as obvious outliers (Taylor and Loescher, 2013).

In response, several software frameworks for automated or semi-automated quality control of environmental time series have emerged. Examples include the metadata-driven GCE Data Toolbox for MATLAB, early web-based systems such as NRAQC for streaming sensor data, and more recently AutoQC4Env and other domain-specific solutions (Sheldon, 2008; Campbell et al., 2013; Kaffashzadeh et al., 2019). The System for automated Quality Control (SaQC) is an open-source framework for traceable and reproducible QC workflows on time series (Schmidt et al., 2023; Schäfer et al., 2023); an overview is provided in Section 4.1, and our ACTRIS-specific wrapper `actris_qc` is described in Section 4.2. While these tools address important aspects of scalability, transparency and automation, they have so far been only sparsely applied to aerosol optical instruments in operational research infrastructures and have rarely been systematically benchmarked against established QA/QC procedures such as those of ACTRIS or GAW.

This paper addresses these needs by presenting, to our knowledge, the first openly documented and fully automated quality-control pipeline for long-term AE33 Aethalometer and Aurora 4000 nephelometer time series that operationalises ACTRIS and GAW guidance in software. Specifically, our approach:

- **formalises expert knowledge and QA/QC recommendations** from ACTRIS, GAW, EPA and European guidance into reproducible, machine-readable QC operators within the SaQC framework, translating narrative guidelines into a standardised, executable workflow;
- **implements an end-to-end automated QC pipeline** for AE33 and Aurora 4000 data that runs both in near-real-time for station operation and on multi-year archives, with full provenance of all tests and transformations;
- **detects and classifies a broad spectrum of data issues**, including outliers, instrument malfunctions, flow and relative-humidity excursions, tape- and optics-related artefacts, noise, plateaus, jumps and gradual long-term drift and fouling;
- **demonstrates cross-site and cross-network transferability** by applying the same operator-based QC logic to urban and regional background stations and by designing the building blocks to be extendable to mid-cost regulatory instruments and low-cost sensor networks; and
- **produces interpretable, AI-ready QC outputs**, providing consistent quality flags and provenance metadata that can be directly consumed by downstream applications such as digital-twin systems, data assimilation frameworks and machine-learning models.

This study presents the first openly documented and fully automated QC pipeline for AE33 and Aurora 4000 time series that operationalises ACTRIS and GAW guidance in software. We formalise expert knowledge and established procedures into modular, machine-interpretable QC operators that can run in real time and on multi-year archives. In contrast to existing instrument- or network-specific workflows, the proposed system is generic by design and scalable across research-infrastructure, regulatory and low-cost sensor networks. The resulting flags and provenance metadata provide an interpretable, transferable and AI-ready foundation for harmonised aerosol optical data streams.

2 Background and state of the art

2.1 QA/QC frameworks in atmospheric research infrastructures

The WMO Global Atmosphere Watch (GAW) programme provides an overarching quality-assurance framework for atmospheric composition observations. GAW Report No. 227 synthesises aerosol measurement procedures, guidelines and recommendations, including core aerosol variables, data quality objectives, recommended inlet and conditioning systems, and instrument-specific calibration and maintenance procedures (World Meteorological Organization (WMO), 2016; Laj et al., 2020). The report emphasises that quality control of data is primarily the responsibility of the station or data originator and describes general principles for identifying and flagging suspect data, but does not define a concrete, standardised software implementation for automated QA/QC of time series (World Meteorological Organization (WMO), 2016).

ACTRIS builds directly upon GAW principles and extends them for European research infrastructures. ACTRIS handbooks and deliverables provide measurement guidelines and standard operating procedures for a wide range of aerosol variables,

https://doi.org/10.5194/egusphere-2026-235
Preprint. Discussion started: 13 March 2026

including AE33 Aethalometer and Aurora 4000 nephelometer measurements (ACTRIS-2 Consortium, 2017b; ACTRIS CAIS-ECAC, 2026; Laurita et al., 2025). Dedicated ACTRIS ECAC guidelines for manual QC of AE33 and Aurora 4000 prescribe instrument configurations, recommended checks (e.g. flow, temperature, RH), and manual inspection of level-0 and level-1 time series, including the generation of temporary higher-level products during the QC workflow (Müller and Fiebig, 2020, 2021). For filter absorption photometers more generally, ACTRIS and RI-URBANS guidance documents describe harmonised approaches to convert eBC to absorption coefficients, apply multiple-scattering and filter-loading corrections, and derive harmonised eBC mass concentrations (Savadkoohi et al., 2024; RI-URBANS, 2024).

In all these documents, QA/QC is conceptualised as a multi-step process that includes instrument intercomparisons, central calibration, site audits, careful documentation and data flagging. However, the actual implementation of QC tests and flag assignments remains in the hands of individual data centres or principal investigators and is typically carried out through a combination of manual inspection and locally developed scripts. There is no common, open-source, software-level realisation of the recommended checks that could be deployed across ACTRIS and GAW stations in a uniform way, nor are the rules expressed in a formal language that would allow automatic execution and provenance tracking (ACTRIS-2 Consortium, 2017a; ACTRIS CAIS-ECAC, 2026).

2.2 QA/QC in regulatory air-quality monitoring

Regulatory air-quality networks operate under their own QA/QC frameworks, largely driven by data quality objectives defined in legislation. The US EPA Quality Assurance Handbook Volume II, for example, outlines a comprehensive QA system for ambient air-quality monitoring programmes, including requirements for siting, calibration and performance audits, collocated measurements, and multi-level data review procedures prior to submission to the Air Quality System (AQS) database (U.S. Environmental Protection Agency, 2026). Similarly, EU guidance and JRC documents describe harmonised protocols for measurement methods, uncertainty assessment, and data validation workflows under the Air Quality Directive, as well as best-practice guides for air-quality plans and model applications (Landgrebe, 2008; European Environment Agency and European Commission Joint Research Centre, 2011; German Environment Agency, 2016).

These frameworks ensure that reported regulatory data meet specified quality objectives and are broadly comparable across jurisdictions. However, they typically stop at the level of procedures and documentation, without defining or providing concrete automated QC pipelines. Data validation is often performed in multi-stage manual processes – such as preliminary automatic screening followed by expert review – using national or regional tools that are not openly specified and that mix instrument diagnostics, meteorological context and policy-driven rules (e.g. special treatment of fireworks, Saharan dust events). As a result, there is limited transparency and interoperability of QC logic even within one jurisdiction, and no direct pathway to re-use these QC concepts in research infrastructures or LCS/citizen-science networks (Clouse, 2024; U.S. Environmental Protection Agency, 2026).

Recent guidance on black carbon monitoring in regulatory contexts, for example within RI-URBANS and European expert groups, focuses on standardising measurement methods, inlet configurations, and data reporting for eBC, but again assumes that data used in analyses have already undergone appropriate QC (RI-URBANS, 2024; Savadkoohi et al., 2024). Automated detection and flagging of instrument artefacts, drift and fouling is generally outside the explicit scope of the regulatory documents.

2.3 Automated QC tools for environmental time series

In parallel with the evolution of QA/QC frameworks, several generic software systems for automated QC of environmental time series have been developed in other domains. The GCE Data Toolbox for MATLAB is a metadata-based framework that supports automated processing, rule-based QC, gap-filling and documentation of environmental datasets, and has been used extensively in long-term ecological research networks and hydrologic observatories. Its rule engine and flagging model inspired later systems, but its reliance on MATLAB and a limited built-in library of QC tests restricts its adoption and extensibility (Sheldon, 2008; Schmidt et al., 2023).

Other examples include the Near-Real Time Autonomous Quality Control (NRAQC) system for streaming sensor data, as well as open-source packages for hydrology and water quality that combine visualisation and automated QC tests (Taylor and Loescher, 2013; Scully-Allison et al., 2018). AutoQC4Env is a more recent system that provides QC services for environmental time series via open web services, again highlighting the need for scalable, machine-readable QC logic in the

https://doi.org/10.5194/egusphere-2026-235
Preprint. Discussion started: 13 March 2026

face of growing sensor networks (Kaffashzadeh et al., 2019). In addition to such generic engines, a number of domain-specific QC algorithms have been developed for particular observing systems. Some related Examples are automated near-real-time QC and cloud screening for AERONET aerosol optical depth or AERONET-OC to retrieval ocean color from radiances measurements (Giles et al., 2019; Zibordi et al., 2022) or QC schemes for satellite and sounding retrievals based on total precipitable water and a-priori error classification (Kwon et al., 2012). For remote atmospheric composition data, e.g. Beck et al. (2022) propose an automated identification of local contamination in otherwise remote time series, using statistical pattern detection and metadata to separate local artefacts from background variability.

A closely related aerosol-domain example is provided by the NOAA/ESRL/GMD Federated Aerosol Network, where the CPD/CPX software environment combines data acquisition, visualisation, event logging and expert data editing within a common operational workflow (Andrews et al., 2019; NOAA Global Monitoring Laboratory, n.d.). The documented QA/QC practice explicitly includes inspection of housekeeping parameters and station event logs, and invalidation or close review of data around span checks, leak checks, filtered-air checks, impactor servicing, filter changes and power interruptions (NOAA Global Monitoring Laboratory, 2022). This event-aware and instrument-aware screening logic provides an important aerosol-specific point of reference for automated QC of optical aerosol time series.

Among generic, reusable frameworks, SaQC is an open-source implementation for traceable and reproducible QC workflows on time series (Schmidt et al., 2023). In this study, SaQC serves as the execution environment (Section 4.1), complemented by the ACTRIS-specific implementation `actris_qc` (Section 4.2); comparable pipelines could in principle be realised with other rule-based QC engines. SaQC has also been integrated into a broader digital ecosystem for FAIR time series data management (Bumberger et al., 2025).

However, most applications of these frameworks and algorithms to date have focused on hydrology, soil moisture, micrometeorology, greenhouse-gas monitoring, and other terrestrial or column-integrated observables, with only rare examples in atmospheric composition monitoring at the level of in-situ aerosol optics. Automated QC methods are rarely tailored to the specific artefacts of optical aerosol instruments such as AE33 and Aurora 4000, and there is little published experience on embedding established aerosol QA/QC guidance (GAW, ACTRIS, RI-URBANS) into such generic QC frameworks.

2.4 Automated QC for air-quality and low-cost sensor networks

The explosion of low-cost air-quality sensor deployments has triggered an extensive body of work on sensor evaluation, calibration and network-level data handling. Reviews of low-cost sensor networks and WMO reports emphasise that LCS can complement reference networks, but that their data are strongly affected by interferences from temperature, relative humidity, cross-sensitivities and sensor ageing, demanding robust QA/QC and recalibration strategies (World Meteorological Organization, 2021; Bagkis et al., 2022; Carotenuto et al., 2023; Bagkis et al., 2025). Numerous studies propose statistical and machine-learning based calibration approaches and ad-hoc QC rules, often tuned for specific sensor types and deployment conditions (Chu et al., 2020; Gualtieri et al., 2024; Hayward et al., 2024).

Beyond calibration-focused work, several studies have developed automated QC algorithms for dense meteorological and air-quality networks. For example, Napoly et al. (2018) and Båserud et al. (2020) exploit spatial and temporal consistency within crowdsourced air-temperature data and operational meteorological networks to flag suspect observations based on neighbourhood statistics and model backgrounds. Wu et al. (2018) introduce probabilistic automatic outlier detection for surface air-quality measurements in China's national network. These approaches typically combine multi-sensor correlation, temporal persistence tests and comparisons to external reference fields or models to assign QC flags, often tightly coupled to a specific network or measurement type.

Despite this activity, there is still no widely adopted, generic QC pipeline that spans the full range from high-end reference instruments to low-cost sensors. LCS papers often implement QC as a bespoke step embedded in the calibration workflow, and sometimes treat regulatory data as "ground truth" without explicitly accounting for their own QC status (World Meteorological Organization, 2021; Okorn and Iraci, 2024; Gäbel and Hertig, 2025). Moreover, lessons learned in LCS QC – such as the importance of dynamic, context-aware thresholds and multi-sensor consistency checks – are rarely propagated back into the QC of research-infrastructure data streams.

In addition, emerging AI-based methods aim to detect anomalies and quality issues in multi-sensor networks using, for example, graph neural networks or other deep learning architectures (Lasota et al., 2025). These methods show promise for

https://doi.org/10.5194/egusphere-2026-235
Preprint. Discussion started: 13 March 2026

identifying subtle multivariate inconsistencies that are difficult to capture with hand-crafted rules but depend critically on high-quality training data and interpretable QC labels. Without a robust, transparent baseline QC pipeline, there is a risk that such models simply learn existing biases or artefacts.

2.5 Instrument-specific QC and harmonisation for aerosol absorption and scattering

A large body of literature addresses the performance, harmonisation and correction of aerosol absorption and scattering instruments themselves. For AE33 and other Aethalometers, studies have investigated filter-loading artefacts, multiple-scattering enhancement factors and wavelength dependence of the correction parameter C for different filter tapes, including cross-sensitivity to scattering (Yus-Díez et al., 2021). Other work has proposed methods to derive dynamic, site-specific C factors from AE33 loading parameters and to compare eBC mass concentrations against MAAP as a reference (Ferrero et al., 2024). Pan-European analyses of long-term eBC measurements have led to recommendations on reporting eBC and its uncertainties, including harmonised conversion from absorption coefficients to mass concentrations and considerations of MAC and C-factor variability (Savadkoohi et al., 2024).

For nephelometers, numerous optical closure studies and ACTRIS deliverables have examined angular truncation, illumination functions, calibration procedures and intercomparisons between Aurora 4000 and other instruments, leading to recommended practices for truncated scattering corrections and RH conditioning (ACTRIS-2 Consortium, 2017b, 2018; Müller and Fiebig, 2020; Teri et al., 2022). Intercomparison campaigns at ACTRIS sites have shown that, when properly calibrated and operated, Aurora 4000 instruments can achieve small inter-instrument biases, but that performance degrades in the presence of fouling, misaligned optics or inadequate RH control (ACTRIS-2 Consortium, 2018, 2019).

These studies and guidelines are essential for understanding and mitigating instrument-specific biases and for harmonising data products across networks. Yet, they typically focus on what should be corrected and reported, not on how to embed this knowledge into fully automated QC pipelines. Implementations often exist as local scripts and individual workflows, are rarely published or documented in detail, and are not expressed in a transferable way that would allow consistent application across many stations and networks. Furthermore, instrument-specific corrections alone do not address generic time-series issues such as missing data, unreasonable spikes, long periods of constant values, or cross-variable inconsistencies (e.g. between absorption, scattering and PM mass).

2.6 Identified gaps and positioning of this work

From this brief review, three gaps become apparent:

1. **Lack of end-to-end automation:** Existing QA/QC frameworks (GAW, ACTRIS, EPA, EU) provide detailed guidance on procedures and data quality objectives, but do not deliver a concrete, open-source implementation that automates the QC of aerosol optical time series in (near-)real time.

2. **Fragmentation across instrument classes and network types:** High-end research infrastructures and regulatory networks largely treat QC separately from low-cost sensor networks and citizen-science deployments, even though the underlying time-series artefacts (outliers, drift, fouling, relative-humidity effects) are similar across instrument classes (Laj et al., 2020; World Meteorological Organization (WMO); United Nations Environment Programme (UNEP); International Global Atmospheric Chemistry project (IGAC), 2024).

3. **Limited availability of machine-readable and reusable QC outputs:** Many published QC approaches do not provide harmonised, machine-readable QC flags and provenance that can be reused consistently across workflows and long time periods. This limits downstream applications that rely on trustworthy baselines (e.g., advanced analytics, automated monitoring, or model–data integration), without these applications being the focus of the QC work itself (Hayward et al., 2024; Lasota et al., 2025).

These gaps are addressed by the contributions outlined in the Introduction: we provide an openly documented, executable and versioned QC rule set and harmonised QC outputs (flags and provenance) for aerosol optical time series, applicable both in real time and on extended historical records. Beyond these overarching gaps, two further aspects are often underrepresented in published aerosol QC schemes: the systematic integration of generic, rule-based QC toolboxes with aerosol-specific guidance (Campbell et al., 2013; Schmidt et al., 2023), and the robust treatment of gradual drift, ageing, and fouling over multi-year

https://doi.org/10.5194/egusphere-2026-235
Preprint. Discussion started: 13 March 2026

periods (Laj et al., 2020; Savadkoohi et al., 2024).

Taken together, these gaps show that the field still lacks a unified, software-level realisation of existing QA/QC guidance for aerosol optical time series. These gaps are addressed by the contributions outlined in the Introduction: we translate GAW/ACTRIS recommendations and instrument expertise into machine-readable rules implemented in the SaQC framework, executable both in near-real time and on extended historical records, and reusable across reference, regulatory and low-cost networks.

In the remainder of this paper, we implement and evaluate this automated QC pipeline for AE33 Aethalometer and Aurora 4000 nephelometer data, building on the conceptual and methodological foundations outlined in Sect. 2. The subsequent sections detail the instruments and sites, the QC logic and parameterisation, and the performance and limitations of the resulting workflow.

3 Instruments and Measurement Sites

This section summarises the main characteristics of the AE33 Aethalometer and Aurora 4000 nephelometer and briefly describes the two ACTRIS sites and datasets used to develop and validate the QC workflow.

3.1 Black Carbon – AE33 Aethalometer

The Aethalometer AE33 (Aerosol Magee Scientific / Aerosol d.o.o., Ljubljana, Slovenia) is a filter-based optical instrument widely used in atmospheric research and air quality applications to determine equivalent black carbon (eBC) concentrations in real time. It operates on the principle of measuring light attenuation caused by aerosol particles collected on a quartz filter tape. The AE33 model represents a significant advancement over earlier single-spot instruments (e.g. AE22, AE31) by introducing a dual-spot technology to compensate for filter-loading effects (Drinovec et al., 2015). For different wavelengths, light is transmitted through two spots on the filter tape simultaneously at different flow rates. By analysing the difference in attenuation between the two spots, the instrument corrects in real time for the nonlinear saturation signal caused by the accumulation of particles – a known source of measurement bias termed the "loading effect" (Drinovec et al., 2015). In total, the AE33 uses seven wavelengths ranging from 370 to 950 nm, allowing for spectral characterisation of aerosol absorption and derivation of diagnostic parameters such as the absorption Ångström exponent (AAE) (Cuesta-Mosquera et al., 2021). The AE33 records a range of primary measurement variables, including

- attenuation (ATN_λ) at each wavelength and spot (e.g. `attn_wavel_spot` with `wavel={w1, ..., w7}` and `spot={sp1, sp2}`);
- uncorrected and corrected eBC concentrations (e.g. `bc_raw_wavel_spot` with `wavel={w1, ..., w7}`, `spot={sp1, sp2}` and `bc1, ..., bc7`);
- flow rates for each channel (e.g. `flow_sp1`, `flow_sp2`, `flow_sum`);
- tape advancement and general instrument status (e.g. `status` and related flags).
- and secondary variables such as temperature, pressure, and humidity in the aerosol inlet or ambient air if external sensors are installed

Appropriate operation of the AE33 requires routine maintenance, including filter tape replacement, flow calibration, and leak checks. Variations in flow on the order of ± 10 or improper sealing can lead to significant under- or overestimation of eBC values, especially at low attenuation levels or during transitions between tape spots (Cuesta-Mosquera et al., 2021).

Intercomparison studies have shown that, when operated under standardised procedures, AE33 instruments demonstrate low unit-to-unit variability and a temporal resolution suitable for both background and urban air quality monitoring (Cuesta-Mosquera et al., 2021). Nonetheless, artefacts such as residual cross-sensitivity to scattering aerosols, filter stabilization (e.g. after changes of relative humidity), and the timing of tape advance events require careful quality-control procedures to ensure data reliability. In the following, we primarily use the eBC concentration at 370 nm from the first wavelength channel (`ebc_w1`) as the target variable for the QC workflow. A frequently used equation for investigating wavelength dependence is given by the absorption Ångström exponent (AAE). The wavelength dependence for eBC concentration is defined for different pairs of wavelengths by the following equations (Moosmüller et al., 2011; Valenzuela et al., 2015):

https://doi.org/10.5194/egusphere-2026-235
Preprint. Discussion started: 13 March 2026

$$AAE_{\mathrm{UVG}} = -\frac{\ln\left(\frac{eBC_{370}}{eBC_{525}}\right)}{\ln\left(\frac{370}{525}\right)} + 1 \qquad AAE_{\mathrm{GR}} = -\frac{\ln\left(\frac{eBC_{525}}{eBC_{880}}\right)}{\ln\left(\frac{525}{880}\right)} + 1 \qquad AAE_{\mathrm{UVR}} = -\frac{\ln\left(\frac{eBC_{370}}{eBC_{880}}\right)}{\ln\left(\frac{370}{880}\right)} + 1. \tag{1}$$

The AAE equations differ from the equations that are often used in aerosol optics, where the ratio of absorption coefficients is used instead of the ratio of eBC. Since the Aethalometer assumes an AAE of unity when converting absorption coefficients to equivalent black carbon, this factor appears as an additive number in the equation.

3.2 Light Scattering – Aurora 4000

The Aurora 4000 polar nephelometer (Ecotech Ltd., Knoxville, Australia) is a three-wavelength integrating nephelometer (blue: 450 nm, green: 525 nm, red: 635 nm) used for measuring various aerosol light scattering properties. The instrument is designed for continuous operation and extends the capabilities of its predecessor, the Aurora 3000 (Müller et al., 2011), by enabling not only the measurement of total and backscattering coefficients, but also multi-angle scattering characterisation in real time. The optical configuration includes a nearly Lambertian light source positioned orthogonally to the detector, producing an angular distribution approximating $\sin(\theta)$, where θ is the scattering angle (Müller et al., 2011).

The angular and spectral resolution of the Aurora 4000 allows for detailed characterisation of aerosol optical properties across 17 discrete angular sectors. These sectors span from a nominal lower angle α to 170°, with α increasing in 5° increments from 10° to 90° (0, 10, 15, …, 90°) (Ran et al., 2023). The instrument's backscatter shutter system enables switching between full-angle and sector-specific scattering measurements, facilitating the calculation of nominal total scattering as well as angle-resolved coefficients.

The angular scattering coefficient $\sigma(\alpha, \lambda)$, measured at wavelength λ and lower angular limit α, can be expressed as

$$\sigma(\alpha, \lambda) = \frac{\lambda^2}{2\pi} \int_0^{180} S(\theta, \lambda) Z(\theta, \alpha)\, d\theta, \tag{2}$$

where $S(\theta, \lambda)$ is the angular scattering function of the aerosol, and $Z(\theta, \alpha)$ represents the illumination function of the instrument. Ideally, $Z(\theta, \alpha)$ follows a sine function for $\theta \geq \alpha$ and is zero otherwise. In practice, this assumption is compromised by factors such as truncation at low and high angles, deviations from Lambertian emission, and beam blockage by the shutter mechanism (Mueller et al., 2012). These instrumental effects must be carefully considered when interpreting scattering measurements.

A more detailed discussion of the physical principles and retrieval limitations of nephelometric measurements can be found in Anderson et al. (Anderson et al., 1996) and Teri et al. (Teri et al., 2022), including a discussion of uncertainty contributions from particle properties. These considerations are essential for the development of robust quality-control routines in automated data-processing pipelines, as pursued in this study within the ACTRIS context. In the following, we primarily use the total scattering coefficient at 450 nm ($\sigma_{\mathrm{sca},450}$; `sca_450`) together with associated instrument state variables as inputs to the QC workflow. A derived quantity for examining the wavelength dependence of the scattering coefficient is the scattering Ångström exponent, which is defined similarly to the AAE.

$$SAE_{\mathrm{BG}} = -\frac{\ln\left(\frac{\sigma_{\mathrm{sca},450}}{\sigma_{\mathrm{sca},525}}\right)}{\ln\left(\frac{450}{525}\right)} \qquad SAE_{\mathrm{GR}} = -\frac{\ln\left(\frac{\sigma_{\mathrm{sca},525}}{\sigma_{\mathrm{sca},635}}\right)}{\ln\left(\frac{525}{635}\right)} \qquad SAE_{\mathrm{BR}} = -\frac{\ln\left(\frac{\sigma_{\mathrm{sca},450}}{\sigma_{\mathrm{sca},635}}\right)}{\ln\left(\frac{450}{635}\right)}. \tag{3}$$

3.3 Data Overview

This study uses time series data obtained from two ACTRIS-compliant in situ aerosol measurement sites operated by TROPOS in eastern Germany: the TROPOS central facility in Leipzig (12°26′3″ E, 51°21′9″ N; 122 m a.s.l.) and the regional

https://doi.org/10.5194/egusphere-2026-235
Preprint. Discussion started: 13 March 2026

background station in Melpitz near Torgau (12°56′ E, 51°32′ N; 86 m a.s.l.).

The TROPOS central facility is located in an urban environment and provides measurements representative of anthropogenically influenced urban conditions. The instruments operated there include the AE33 Aethalometer and the Aurora 4000 Nephelometer. Although the station is not an official ACTRIS station, it is used by the WCCAP (World Calibration Centre for Aerosol Physics), which is hosted at TROPOS, as a facility for testing hardware and software developments for use in the ACTRIS infrastructure.

The Melpitz site is situated in a rural background environment near Torgau (Saxony), approximately 50 km northeast of Leipzig. The station is surrounded predominantly by agricultural land and is only weakly affected by nearby local emission sources. Melpitz represents a TROPOS supersite with a comprehensive set of instrumentation for physical and chemical aerosol and trace gas characterisation. As part of the German ACTRIS network, it complements the urban dataset from TROPOS with measurements reflecting regional background aerosol characteristics. Instruments at Melpitz are operated under the same standardised quality-control procedures.

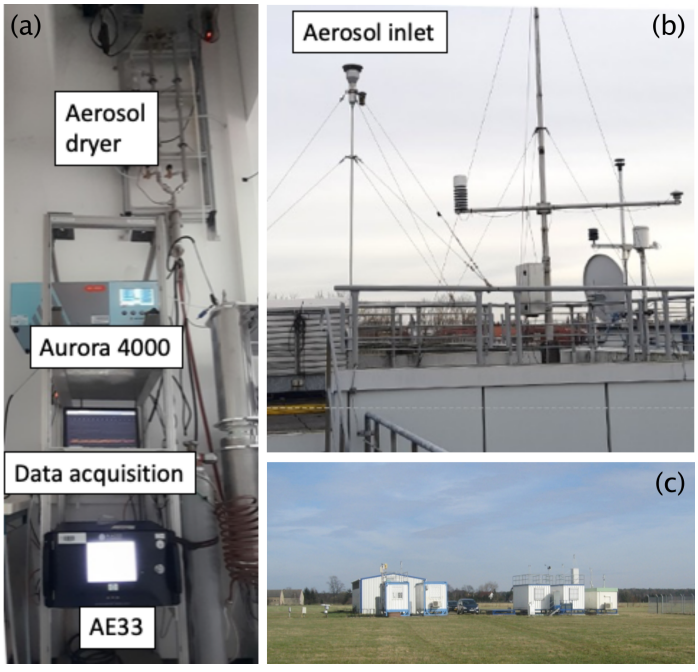

Figure 1. (a) The TROPOS urban measurement site with an Aethalometer, Nephelometer and aerosol conditioning unit. (b) Aerosol inlet on the roof. (c) The Melpitz measurement station from outside. The arrangement of the aerosol inlets and instruments inside the station is similar to that at TROPOS measurement site.

All instruments were operated under standardized conditions, and the data were post-processed using the SaQC-based quality control pipeline described below. The Aethalometer recorded data at intervals of 10, 30, and 60 seconds. Despite these different logging intervals, the internal averaging time of the AE33 was consistently 60 seconds. Consequently, averaging the data to a time resolution of 1 minute within SaQC in the last Stage corresponds to the actual measurement time resolution of the AE33. For nephelometers, data averaged at 10-second intervals were averaged to one-minute intervals by SaQC.

The QC workflow was developed using two years of data collected at the TROPOS urban measurement site, spanning from April 2022 to April 2024, including extended data gaps for the Aethalometer and a system failure for the Nephelometer. Figure 2 illustrates representative data from one channel of each instrument: the Aethalometer's eBC at 370 nm (`ebc_w1`, Fig. 2a) and the nephelometer's scattering coefficient at 450 nm ($\sigma_{\mathrm{sca},450}$; `sca_450`, Fig. 2b). Typical eBC concentrations

https://doi.org/10.5194/egusphere-2026-235
Preprint. Discussion started: 13 March 2026

(ebc_w1) were below 2 µg m^{-3}, with episodic peaks occurring every few weeks reaching 6–8 µg m^{-3} and, less frequently, values up to 10–14 µg m^{-3}. Due to large data gaps during the summers of 2022 and 2023, seasonal trends could not be robustly identified. Mean daily values of the nephelometer scattering coefficient ($\sigma_{sca,450}$; sca_450) generally remained below 100 Mm^{-1} in summer, whereas wintertime measurements exhibited more pronounced variability with peaks reaching up to 300 Mm^{-1} every few weeks. A system failure, likely caused by instrument clogging, occurred in autumn 2023 and resulted in highly erratic data until the device was replaced and restarted operation in February 2024.

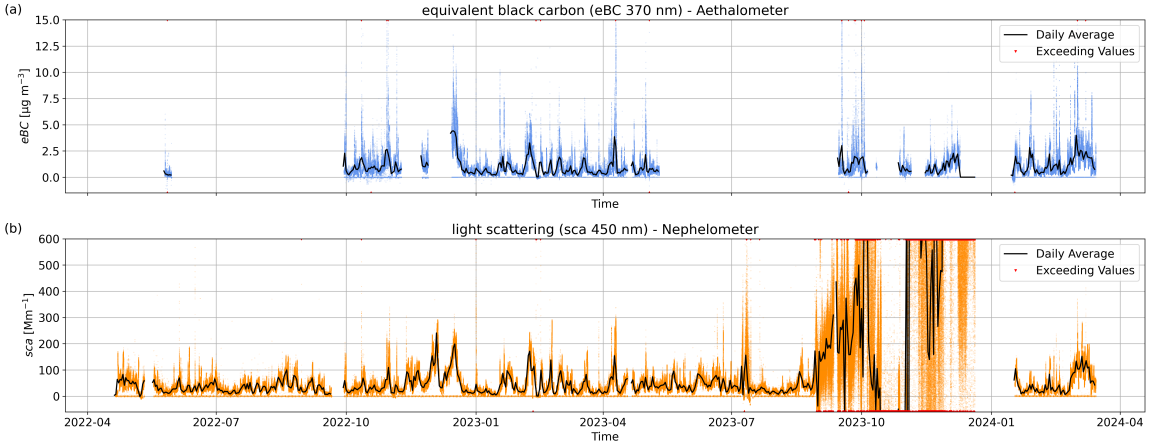

Figure 2. Data from the TROPOS measurement site in Leipzig, Germany. (a) AE33 Aethalometer data as equivalent black carbon (eBC) of the first channel at 370 nm (ebc_w1). (b) Light-scattering data from the first channel of the Aurora 4000 nephelometer at 450 nm ($\sigma_{sca,450}$; sca_450).

The developed QC solution for the TROPOS urban measurement site was validated with data from the rural measurement site Melpitz ranging from November 2024 to April 2025 (Fig. 3). Daily mean Aethalometer records for black carbon (ebc_w1) were mostly below 2 µg m^{-3}, while multi-day pollution episodes occurred in November and late December 2024 with values up to 4–8 µg m^{-3}. From February 2025 onwards the variability of the signal increased, with several pronounced peaks between 4 and 6 µg m^{-3}. The temporal evolution of the nephelometer's scattering coefficient ($\sigma_{sca,450}$; sca_450) closely followed the eBC time series, with standard values below 100 Mm^{-1} and peaks up to about 300 Mm^{-1} in November 2024 and spring 2025.

Besides the primary variables shown, both instruments record several additional data series accompanying the main measurements, many of which have been utilized in the quality control (QC) process. Representative images of these auxiliary data series are provided in the uploaded QC results (Houben et al., 2026a).

4 Quality Control Framework

4.1 SaQC Software

The SaQC software (System for automated Quality Control) is a general-purpose, open-source framework designed to support automated, reproducible and transparent quality control (QC) of time series data across environmental domains. SaQC was developed explicitly to enable traceable and reproducible data streams in environmental science and to serve as a core component of FAIR (Findable, Accessible, Interoperable, Reusable) data workflows by making QC processing steps machine-readable and versionable (Schmidt et al., 2023).

A central design principle of SaQC is its domain-agnostic and low-code configuration concept. Instead of hard-coding procedures for specific applications, QC rules are defined in structured configuration files that describe condition-based checks (e.g. range tests, temporal consistency, handling of missing values, compound flagging strategies). This strict separation between rule definition and execution allows domain experts to encode their expertise directly, without changing the core

https://doi.org/10.5194/egusphere-2026-235
Preprint. Discussion started: 13 March 2026

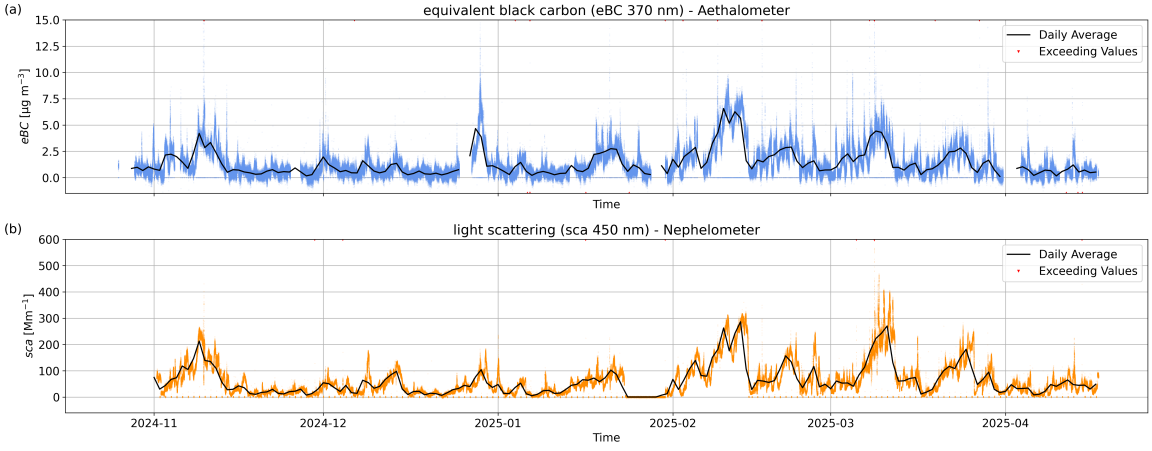

Figure 3. Data from measurement site at Melpitz measurement site, Germany. (a) AE33 Aethalometer data as equivalent black carbon (eBC) of first channel at 370 nm (`ebc_w1`). (b) Light scattering data from first channel of Nephelometer Aurora 4000 at 450 nm ($\sigma_{\mathrm{sca},450}$; `sca_450`).

software and largely without programming. The same configuration can be applied to historical archives, to live data streams and, if version-controlled, can be re-used and adapted across projects and research infrastructures.

Beyond classical threshold-based validation, SaQC provides a comprehensive library of generic pre- and post-processing routines (e.g. resampling, detrending, interpolation) and QC tests ranging from simple range or variance checks to more advanced methods such as change-point detection, pattern recognition and multivariate anomaly detection. In addition, SaQC natively supports the integration of machine learning (ML) techniques, including unsupervised anomaly detection, multivariate pattern recognition and graph-based models. This extensibility enables hybrid QC workflows in which rule-based and ML-based strategies complement each other and can be tuned to specific instruments, sites or network-level requirements (Lasota et al., 2025).

A distinctive feature of SaQC is its explicit and flexible handling of quality flags. Users can define arbitrary flagging schemes (e.g. *good*, *suspicious*, *bad*, *maintenance*) and control how flags propagate through the processing chain. SaQC keeps a full *flag history* by storing, for each data point, which QC test produced which flag. This allows (i) the reconstruction of the effective decision logic a posteriori, (ii) the aggregation or translation of heterogeneous flagging schemes from different data providers into harmonised quality indicators and (iii) robust resampling of both data and flags in a consistent way. In combination with metadata enrichment and version control of configuration files, this provides the technical basis for FAIR data streams and reproducible QC pipelines across sites and instrument classes.

SaQC can be operated via a command-line interface, a Python API or a web-based configuration application. This makes it suitable both for exploratory development (e.g. interactive tuning of QC rules on individual time series) and for fully automated, near-real-time operation in production data pipelines. The software is designed to be integrated with standard workflow and scheduling tools (e.g. `cron` jobs or workflow engines) and with higher-level information systems such as time-series databases, sensor management systems or research data portals (Bumberger et al., 2025). In this way, QC becomes an explicit, traceable component of the end-to-end data lifecycle, rather than an opaque post-processing step. For high-frequency and real-time applications, SaQC supports fully automated execution. It can be run in batch mode or as a service integrated into live data acquisition pipelines, making it suitable for research infrastructures like ACTRIS, where operational consistency and scalability are required across diverse stations and instrument types (ACTRIS-2 Consortium, 2018).

In the context of this study, SaQC is applied to aerosol time series from AE33 Aethalometers and Aurora 4000 nephelometers at two ACTRIS sites. Instrument-specific QC rules are implemented to capture known issues such as flow instability, attenuation saturation, scattering anomalies and artefacts in derived intensive parameters such as the absorption Ångström exponent

https://doi.org/10.5194/egusphere-2026-235
Preprint. Discussion started: 13 March 2026

(AAE) and scattering Ångström exponent (SAE). All QC logic is encoded in python files, and the resulting pipelines are fully automated, version-controlled and re-runnable. This ensures that the aerosol optical data streams used here are not only quality-controlled in real time, but also FAIR-compliant, transparent and reproducible across ACTRIS National Facilities and beyond.

4.2 ACTRIS Specific QC Solution

While SaQC offers a flexible, general platform for automated quality control, ACTRIS has specific operational needs, such as harmonised database structures, standardised flagging schemes and support for multiple atmospheric instruments operated in a distributed research infrastructure. To address these additional demands, the `actris_qc` Python package was developed as an ACTRIS-tailored solution (Fig. 4). It builds directly on SaQC's core functionalities but adds ACTRIS-specific workflows, tuned QC parameters and data-access routines for ACTRIS instruments. In this way, `actris_qc` translates the generic, rule-based SaQC concept into a deployable, station-level QC pipeline that produces reproducible, FAIR-compliant aerosol data streams across the ACTRIS network.

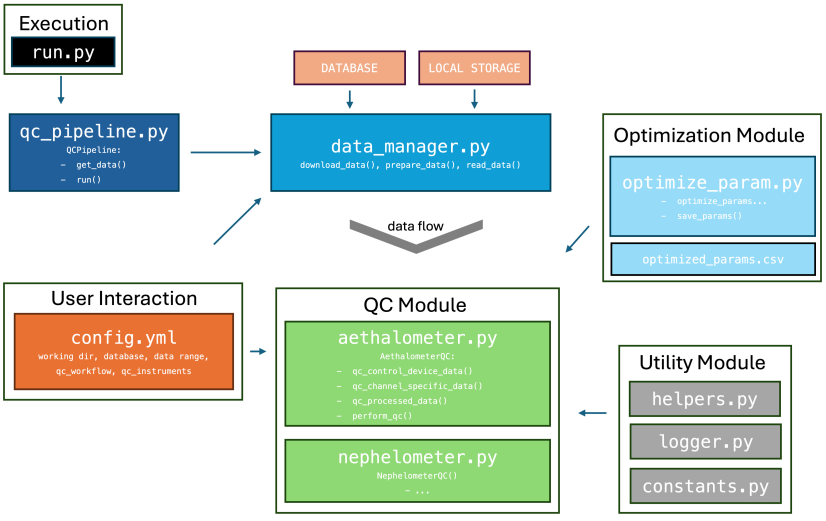

Figure 4. Schematic overview of the `actris_qc` Python package wrapped around SaQC functionalities for seamless integration at ACTRIS measurement stations. Systems integrators can obtain the package from a public repository (see Data and Code Availability) and install it using standard Python tools. Only the `config.yml` file needs to be adjusted to reflect the local database configuration and the desired execution frequency of the automated quality-control workflow. The `run.py` script should then be executed regularly on the station's operating system to trigger the QC.

A key element of this translation is the way `actris_qc` exploits SaQC's flexible flagging and configuration concept. The flagging scheme with its well-defined categories (e.g. `GOOD`, `DOUBTFUL`, `BAD`) is encoded once in the SaQC configuration and then applied uniformly across instruments and sites. Numeric codes, human-readable labels and their semantics are defined in machine-readable form, so that each QC test in SaQC can assign flags that are directly compatible with ACTRIS standards. This makes it possible to fully benefit from the ACTRIS flagging recommendations without adding instrument-specific code, and it ensures that quality information is comparable across stations and time. At the same time, the underlying mechanism remains generic: other networks or projects can adopt the same QC workflows by providing their own flag dictionaries and minimal configuration changes, without modifying the implementation of `actris_qc` or SaQC.

The `actris_qc` package is designed as a modular system that allows straightforward integration of additional devices while preserving the standardised ACTRIS local database structure. Station operators execute the main script `run.py` at

https://doi.org/10.5194/egusphere-2026-235
Preprint. Discussion started: 13 March 2026

regular intervals on local machines that collect the instrument data. This script orchestrates the full QC workflow: it retrieves new data from the local database (or from local files), applies the configured SaQC-based QC procedures and generates diagnostic plots, CSV outputs and QC logs. Once scheduled (e.g. via `cron` or similar tools), this enables continuous, unattended quality control in near real time.

Configuration of the system is concentrated in a single file, `config.yml`, where database credentials *must* be specified and QC settings *can* be adapted. Besides database connectivity, the configuration also defines which instruments are active at a station, which QC workflow should be applied, and how far back in time the system should look for new or updated records. The solution also supports data retrieval from local files for experimental or offline quality control. While modifications to the underlying SaQC configuration are possible, we recommend using the parameter sets determined and validated in this study as default settings to ensure robust and comparable results across sites. Instrument-specific QC logic is implemented in the `qc` module, which currently provides dedicated workflows for AE33 Aethalometer and Aurora 4000 nephelometer data. The modular structure ensures that additional instruments can be incorporated with minimal additional code by re-using the same SaQC abstractions. In practice, transferring the solution to another ACTRIS station, or even to another network with a different database layout, mainly requires adapting the configuration and data-access layer rather than redesigning the QC logic.

The system applies the SaQC flag handling to classify data points into categories such as `GOOD`, `DOUBTFUL` and `BAD`, thereby providing a harmonised quality descriptor for downstream users. The `actris_qc` package also includes a parameter optimisation workflow to derive appropriate settings for individual QC methods from reference datasets. An example of this optimisation procedure is implemented in the `optimization` module, and precomputed, recommended parameter sets are stored in CSV files. This allows stations to directly adopt well-tested QC configurations while retaining the option to recalibrate thresholds for local conditions if needed.

Across all local installations at measurement sites, the ACTRIS database structure remains consistent, ensuring seamless integration and interoperability of the developed solution. The `data_manager.py` module encapsulates data access and storage, handling efficient retrieval from databases or local files and exports QC results as data and flags for further analysis and upload to ACTRIS data infrastructures. Together, these components turn SaQC's generic quality-control concepts into an operational, reusable and transparent QC solution that can be deployed uniformly across ACTRIS National Facilities, while remaining transferable to other environmental monitoring networks through configuration-level adaptations.

5 QC Logic and Implementation

5.1 Quality Control Pipeline

The quality control workflow for atmospheric measurement devices within the `actris_qc` package follows consecutive steps to ensure the production of a final, quality-assured data set (Fig. 5). Initially, after the raw data records from the considered instruments are obtained, they are filtered for relevant variables and temporally aligned to a common interval (i.e. every 10 s), followed by the flagging of missing values. Quality control then begins with device-level checks (Stage 1) – such as assessments of temperature, pressure, and flow – which generate flags affecting the source variables and are subsequently propagated to the variables of interest (or primary variables), i.e. the equivalent black carbon eBC and light scattering coefficient σ_{sca} series.

Subsequent channel-specific checks (Stage 2) are applied, where the primary variables eBC and σ_{sca} and channel-specific attenuation are checked, with flags assigned only to the respective channels. All flags from these steps are concatenated while realigning the data back to the original grid, before being resampled to a coarser temporal resolution (1 min, arithmetic mean). In Stage 3, derived variables are then calculated and subjected to further QC checks tailored to these variables (i.e. absorption and scattering Ångström exponents AAE and SAE). During this sequential approach, each step is logged through an extensive protocol, and both intermediate and final QC results are exported as figures and data files, resulting in a comprehensive and transparent QC documentation.

By structuring the pipeline into these three stages – from device control variables via channel-specific checks to derived diagnostics – the workflow closely mirrors the stepwise screening recommended in established QA/QC guidelines (e.g. World Meteorological Organization (WMO) (2016); Müller and Fiebig (2020, 2021); ACTRIS CAIS-ECAC (2026); U.S. Environmental Protection Agency (2026)), but expresses them as explicit, machine-readable rules within SaQC and `actris_qc`.

https://doi.org/10.5194/egusphere-2026-235
Preprint. Discussion started: 13 March 2026

This enables reproducible, FAIR-compliant aerosol data streams that can be transferred across stations and instruments with minimal reconfiguration.

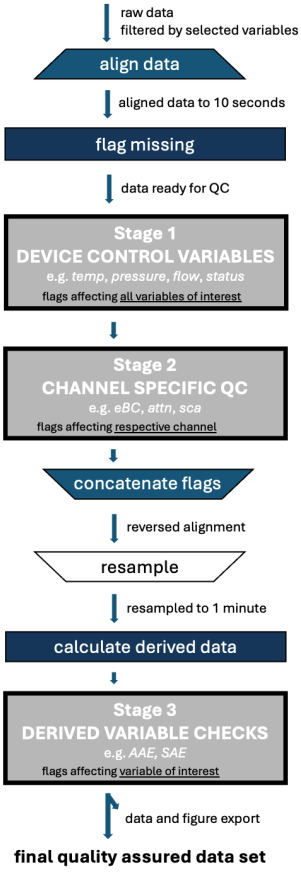

Figure 5. Schematic overview of the quality control workflow developed for the Aethalometer and Nephelometer atmospheric instruments.

5.2 Event Classification

The raw datasets of the primary variables of the first channels (`ebc_w1`, `sca_450`) from the TROPOS and Melpitz measurement sites (Fig. 2 and Fig. 3) exhibit various anomalies identified through visual inspection. For both instruments and sites, specific time periods were selected to represent each anomaly category. Table 1 lists the identified anomalies, their corresponding time ranges, and brief descriptions. The most frequent anomalies include

- exceptionally high values and local outliers,
- increased scattering or noise,
- nearly constant records below the instrument's detection limit/noise,
- sudden jumps followed by device events (e.g. filter change),
- doubtful AAE and SAE fluctuations after filter change,
- unreasonably low values or unreasonable peaks.

https://doi.org/10.5194/egusphere-2026-235
Preprint. Discussion started: 13 March 2026

Each anomaly from the TROPOS measurement site for both instruments was isolated and subjected to quality control. According to the characteristics of the anomalies, suitable SaQC methods and functions were selected, properly parameterized, and implemented in the QC pipeline. Next, resulting flags (`DOUBTFUL` and `BAD`) for data points within the selected time ranges were visualized and checked for consistency across all anomalies. The developed QC workflow, including the obtained parameterization, was finally validated with data from the Melpitz station. A list of all incorporated tests and their corresponding parameterization for both instruments is attached in the Appendix (Table A1 and A2).

This anomaly-based event classification step plays a similar role to the manual inspection recommended in GAW and ACTRIS guidelines, but here it is explicitly used to tune and validate the automated SaQC operators for aerosol-specific artefacts.

5.3 Stage 1: Device Control Variables

Device control variables include status flags and environmental readings such as temperature, pressure, and flow rates. For the AE33 Aethalometer, three independent flow rates (spot 1:`flow_1`, spot 2: `flow_2`, sum: `flow_c`) as well as the inlet relative humidity (`rh_inlet`) were continuously monitored. Flags were assigned when values deviated from expected operational ranges:

- `flow_1`: [3.7–4.05] $\mathrm{L\,min^{-1}}$ (outside → `BAD`)
- `flow_2`: [0.8–1.3] $\mathrm{L\,min^{-1}}$ (outside → `BAD`)
- `flow_c`: [4.8–5.0] $\mathrm{L\,min^{-1}}$ (outside → `BAD`)
- `rh_inlet`: [0–50] % (outside → `BAD`)
- `rh_inlet`: [40–50] % (inside → `DOUBTFUL`)

Device status variables (e.g. `status_inst`, `status_ctrl`, `status_led`, `status_valve`, `numflag`) that are not equal to 0 indicate malfunctions or provide information about the operating status that does not affect data quality. The status information has been interpreted according to the manufacturer's logic and identified as necessary. Numflag is not a standard output of the AE33. It was used during operation of the device to indicate periods of maintenance work, among other things.

- `status_valve` $\neq 0$: 5-minute backfill flag propagation (`DOUBTFUL`),
- `status_valve` $\neq 0$: 30-minute frontfill flag propagation (`BAD`).

For the Aurora 4000 Nephelometer, the inlet temperature, pressure and humidity were recorded. The data ranges for relative humidity were set to the same range intervals as those employed for the AE33 Aethalometer. Pressure and temperature ranges were set as follows:

- `temp_int`: [233.15–313.15] K (outside → `BAD`)
- `pres_int`: [950–1030] hPa (outside → `BAD`)

Device status variables (`state_major` and `state_dio`) for the Nephelometer were monitored to assess system condition. Values deviating from zero were flagged as `BAD` data points. Additionally, flag propagation from `state_major` was applied with a 5-minute backfill flagged as `DOUBTFUL` and a 20-minute frontfill flagged as `BAD`.

The Stage 1 checks explicitly encode the instrument-operation and inlet-conditioning requirements described in GAW aerosol guidelines and ACTRIS ECAC manual QC for AE33 and Aurora 4000 (e.g. flow tolerances, inlet RH $< 40\,\%$, interpretation of device status flags). Deviations from these recommended ranges are mapped to the flag categories `GOOD`/`DOUBTFUL`/`BAD`, thereby providing a software-level realisation of the narrative guidance in these documents and enabling a consistent application of the flagging scheme across stations.

5.4 Stage 2: Channel-Specific Quality Control

Primary variables such as attenuation for the first spot (`attn`), equivalent black carbon concentration (eBC), and scattering coefficients (σ_{sca}) were subject to individual range and consistency checks. Both devices measure on multiple channels with different wavelength detectors, and each channel was quality controlled separately by applying the following tests.

For the AE33 Aethalometer, the following ranges for attenuation were set:

https://doi.org/10.5194/egusphere-2026-235
Preprint. Discussion started: 13 March 2026

- `attn`: [0–120] (outside → `BAD`)
- `attn`: [80–100] (inside → `DOUBTFUL`)

Multiple tests were applied to the black carbon series. First, a noise detection with the SaQC function `flagByScatterLowpass` was applied using optimized parameters (Section 5.7). Consecutive range tests considering the lower detection limit of the device and plausible maximum values limited upper and lower bounds:

- eBC: [-0.075–100] µg m^{-3} (outside → `BAD`)
- eBC: [-0.075–0.05] or [20–100] µg m^{-3} (inside → `DOUBTFUL`)

Next, a test was conducted to identify implausible periods characterized by minimal data variation, remaining below the instrument's inherent measurement noise, with a threshold set at 0.012 µg m^{-3} and a window size of 12 minutes. Finally, remaining outliers were removed from the series with a LOF (local outlier factor) test (threshold: 1.17, number of values: 400) in combination with a 1-hour rolling mean to remove only outliers pointing towards smaller values than the rolling mean (downward spikes).

For the Aurora 4000 Nephelometer, similar quality tests were applied to the σ_{sca} data. First, standard range tests were used to constrain reasonable data ranges, with thresholds set as follows:

- σ_{sca} values: [0–20 000] Mm^{-1} (outside → `BAD`)
- σ_{sca} values: [0–0.05] Mm^{-1} or [6 000–20 000] Mm^{-1} (inside → `DOUBTFUL`)

The upper limit of the `BAD` data range corresponds to the detection limit, while the lower threshold of the `DOUBTFUL` data range is determined by the instrument's noise level. The upper threshold of the `DOUBTFUL` data range was calibrated based on events recorded during the data collection period in urban settings and during New Year's Eve (Khedr et al., 2022).

Flats and constant values were flagged with a threshold of 0.012 and a window size of 12 minutes. Finally, noise detection was performed in order to identify data periods with increased noise, where all matching data points were flagged as `DOUBTFUL`.

The Stage 2 range and variability checks correspond to the generic time-series screening procedures recommended in GAW aerosol guidelines and in regulatory QA handbooks (range tests, spike and noise detection, persistence tests). Within SaQC and `actris_qc`, these concepts are implemented as explicit operators with ACTRIS-compatible flags (`GOOD`, `DOUBTFUL`, `BAD`), turning the narrative notions of automatic screening and data review into a reproducible rule set that can be re-used across instruments and sites.

5.5 Stage 3: Derived Variable Checks

After performing quality checks on device control and channel-specific variables, the variables of interest (eBC, σ_{sca}) were resampled to a 1-minute resolution (arithmetic mean), retaining only data points that passed the previous QC stages. Based on the remaining data, three absorption Ångström exponents (AAE) were calculated from the eBC signals, each using different wavelength ratios as defined in Equation 1:

First, a range test was applied to each AAE series and flags were assigned for the following limits:

- $AAE < 0.8$ or $AAE > 2.2$ → `DOUBTFUL`,
- $AAE < 0.5$ or $AAE > 3.0$ → `BAD`.

Subsequently, a discrepancy check was conducted, where a parameter defining the tolerated absolute difference between the three AAE series was set to 0.7:

- $AAE_{\mathrm{UVG}} \gg AAE_{\mathrm{UVR}}$ or $AAE_{\mathrm{UVR}} \gg AAE_{\mathrm{GR}}$ → `BAD`.

The criteria listed above are applicable to the measurements taken at Melpitz and TROPOS. When applying them to European wide monitoring networks, the thresholds should be derived from a re-analysis of historical data to ensure suitability for all

https://doi.org/10.5194/egusphere-2026-235
Preprint. Discussion started: 13 March 2026

measurement sites and aerosol types. A more comprehensive analysis that combines multiple datasets would be required for this, but it lies outside the scope of the current manuscript.

For the Aurora 4000 Nephelometer, a similar approach as for the Aethalometer was implemented. Three scattering Ångström exponents (SAE) were calculated from the resampled σ_{sca} signals according to Equation 3. A discrepancy check for the Nephelometer was applied according to the same rules as for the Aethalometer, but the tolerated difference was set to 1.0. Limits for AAE and SAE were set based on the processed data sets from the TROPOS measurement site as well as supported by studies from Suchánková et al. (2024); Zhao et al. (2021).

The use of AAE and SAE as diagnostic quantities follows ACTRIS guidance, where these derived products are inspected during manual QC to identify residual artefacts (e.g. loading, scattering cross-sensitivity, RH effects). By embedding these checks as Stage 3 operators in SaQC and propagating their flags back to the primary variables, we effectively automate this diagnostic step and make the resulting decisions traceable and reproducible within the ACTRIS flagging framework.

5.6 Post QC loading compensation evaluation

In the following, we will outline the use of SaQC in an operational scientific context using an example. Loading effects of an AE33 can be investigated using statistical analysis after the time series adjusted with SaQC have been analyzed in an offline or semi-online process of instrument-specific analyses, as described in (Drinovec et al., 2015). One method, following Drinovec et al. (2015), is to represent the eBC concentrations in bins of the attenuation (ATN) for a long time series (see Figure B1). Statistically, values for eBC concentration and the loading state of a filter spot reflected by ATN are uncorrelated, provided that no artifacts occur, e.g., filter changes are always performed at the same time of day, resulting in a correlation with the daily cycle of the eBC concentration. Based on the two eBC concentrations at different wavelengths, it can be seen that there is a slight dependency for the two channels in the UV (channel 1, ebc_w1) and NIR (channel 6, ebc_w6). For the measurements at TROPOS, UV and NIR eBC are positively correlated with ATN, and for Melpitz they are negatively correlated. This result indicated a station-specific loading effect. However, wavelength dependencies reflected by the AAE are mutually compensated for Melpitz and TROPOS. Limits for flagging the AAE proved to be favourable for the Melpitz and TROPOS stations. In a large network with different aerosol types and concentrations, these limits must be re-evaluated, also with regard to loading effects.

Due to its degree of automation, SaQC not only provides automatic statistical analyses in real time, but also allows archived data sets to be accessed and subjected to a uniform, traceable QC method. This ensures, e.g., the reanalysis of large datasets.

5.7 Parameter Optimization

Multiple sections with increased noise were detected for both instruments at the TROPOS measurement site. In order to find optimal parameters for SaQC's `flagByScatterLowpass` test, which is typically applied for noise detection, a separate preceding workflow was executed. In a first step, regions of increased noise were flagged manually using SaQC's `flagByClick` functionality. The manually selected data points were used as targets for the optimization process, which automatically determined parameters for the `flagByScatterLowpass` test. The resulting parameters for `ebc_w1` and `sca_450` were stored as CSV files and were loaded during the main QC pipeline of the respective device. Noise detection can be switched on and off in the configuration files and was only applied for the TROPOS site.

This parameter optimization reconciles generic SaQC operators with instrument- and site-specific behaviour, in line with QA/QC guidelines that recommend local tuning and validation of automatic screening rules against expert judgement.

5.8 Flag Propagation and Finalization

Flags generated at the device control level were transferred the variables of interest, i.e. to the first channel of equivalent black carbon from the Aethalometer and to the first scattering channel from the Nephelometer. Flags generated specifically for a channel from the variables of interest remained on that channel and were not further transferred to other series. The flags from the channel-specific attenuation were transferred similarly, for each channel, to the corresponding variable of interest.

The data from the variables of interest were resampled to 1-minute intervals using the arithmetic mean. Only data points passing all QC stages were retained for the integrated analysis, and the results were written to two files. The first dataset contains results from the original data on the measured grid, including information about the flags, while the second dataset comprises the resampled data along with flag information.

https://doi.org/10.5194/egusphere-2026-235
Preprint. Discussion started: 13 March 2026

After each individual test, a figure is saved in the working directory visualizing the impact of the respective test on the data, enabling transparency throughout the steps of the QC pipeline. Together with the explicit storage of all flags and their provenance in SaQC, this design supports traceable, FAIR-compliant QC workflows and aligns with the recommendations of major QA/QC frameworks to document both data and processing history.

6 Application and Results

This section presents the identified anomalies, demonstrates the outcome of the full QC pipeline for both instruments at the TROPOS measurement site, illustrates selected special cases, and shows the validation with the Melpitz data sets. Finally, we summarise flag statistics and computational performance for the selected anomalies.

Both devices operate on multiple wavelength channels. In the following, we focus on the first channel of each instrument, corresponding to the shortest wavelength (`ebc_w1`, `sca_450`), which is most relevant for downstream analyses and provides a compact view of the QC behaviour.

6.1 Aethalometer

Stages 1 and 2 of the QC workflow combine device-control information with channel-specific tests for the variable of interest `ebc_w1`. Figure 6a illustrates the resulting flags for the Aethalometer at the TROPOS site for anomaly bc2 after completion of Stage 2 and concatenation of all flags. Several QC tests are triggered along the workflow. Most downward spikes are captured by the range tests on the primary variable `ebc_w1`, with the majority classified as `BAD` and a smaller fraction as `DOUBTFUL`. Remaining downward spikes are associated with device-specific events (e.g. changes in `status_inst` related to filter changes). Flag propagation around `status_valve` events marks preceding records as `DOUBTFUL` and the anomalously high records following such events as `BAD`. Residual downward spikes that are not linked to device status are finally removed by the local outlier test.

Following Stages 1 and 2, derived-variable checks are applied in Stage 3. Channel-specific AAE values are calculated and their mutual consistency is evaluated according to the logic described in Section 5.5. The resulting series and flags are shown in Fig. 6b. Several high and low peaks in the AAE series are identified and flagged, as well as two time periods with increased noise, where the discrepancy tests mainly flag the higher values and the range tests the lower values. Figure 6c visualises the combined result of Stages 2 and 3, where all flags from Stage 3 have been transferred back to the variable of interest `ebc_w1`. This step reveals additional downward spikes and low-value intervals with enhanced AAE variability that were not detected in the earlier stages.

Figure 6d compares the original `ebc_w1` series with the final cleaned time series, where all data points flagged as `BAD` or `DOUBTFUL` have been removed. Downward outliers and implausible value ranges are effectively eliminated, and the cleaned series is subsequently resampled to a 1-minute resolution (arithmetic mean) for further analyses.

6.2 Nephelometer

Analogous to the Aethalometer workflow, Fig. 7a shows the flags for the Aurora 4000 Nephelometer at the TROPOS site after Stage 2 and concatenation of all flags for anomaly bc1, for the variable of interest `sca_450`. In this case, only two pronounced anomalies are detected, both associated with a device-control event and the corresponding flag propagation window (`DOUBTFUL`).

Figure 7b presents the scattering Ångström exponents SAE derived from multiple channels together with the resulting flags. Periods of increased noise as well as exceptionally high peaks in SAE are flagged by the range and discrepancy tests. Transferring these flags to the `sca_450` series (Fig. 7c) captures remaining downward spikes that were not removed in Stage 2. The final cleaned and resampled `sca_450` signal is shown in Fig. 7e.

6.3 Exemplary Special Cases

In contrast to the previous subsections, which present the full QC pipeline for representative anomalies and time ranges, this subsection briefly illustrates a special case of a rare anomaly.

https://doi.org/10.5194/egusphere-2026-235
Preprint. Discussion started: 13 March 2026

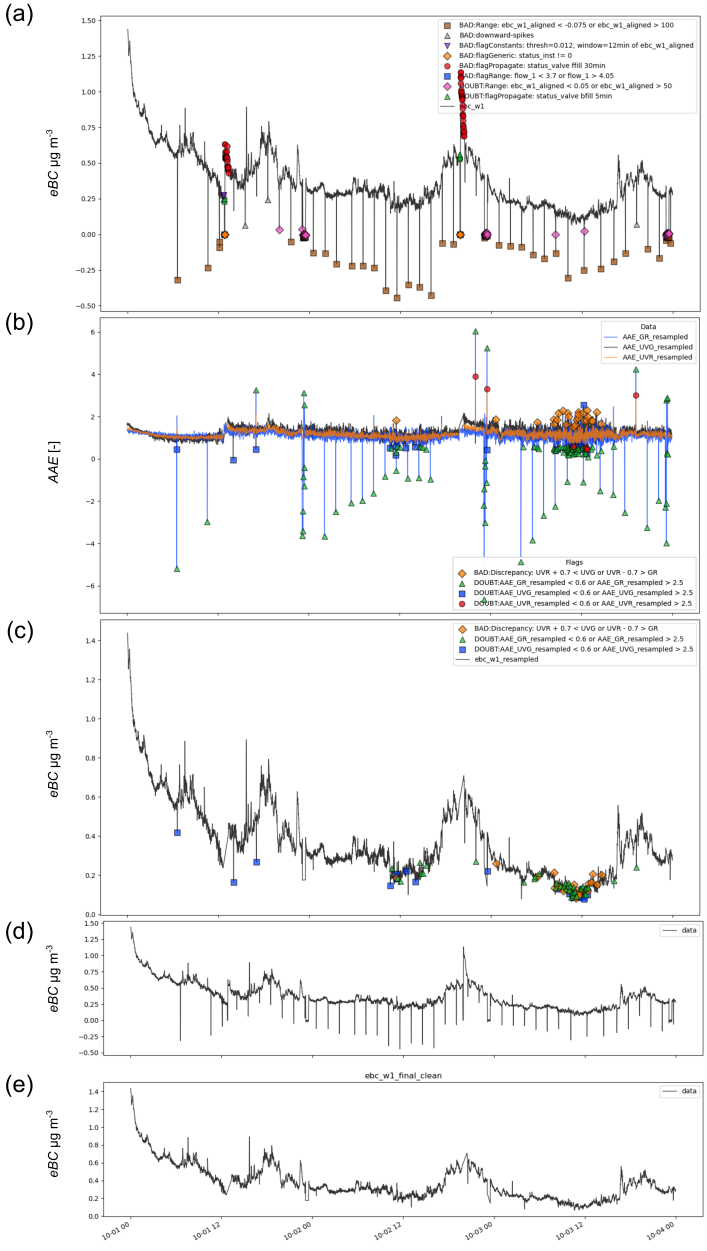

Figure 6. Resulting QC flags for `ebc_w1` measured by the AE33 Aethalometer at the TROPOS measurement site for anomaly bc2. (a) Flags after Stage 2 (channel-level QC of `ebc_w1`), (b) flags from QC tests applied to the derived AAE time series (Stage 3), (c) Stage 3 flags propagated back to the final variable of interest `ebc_w1`, (d) original `ebc_w1` series, (e) final, cleaned `ebc_w1` series after applying the aggregated flags.

https://doi.org/10.5194/egusphere-2026-235
Preprint. Discussion started: 13 March 2026

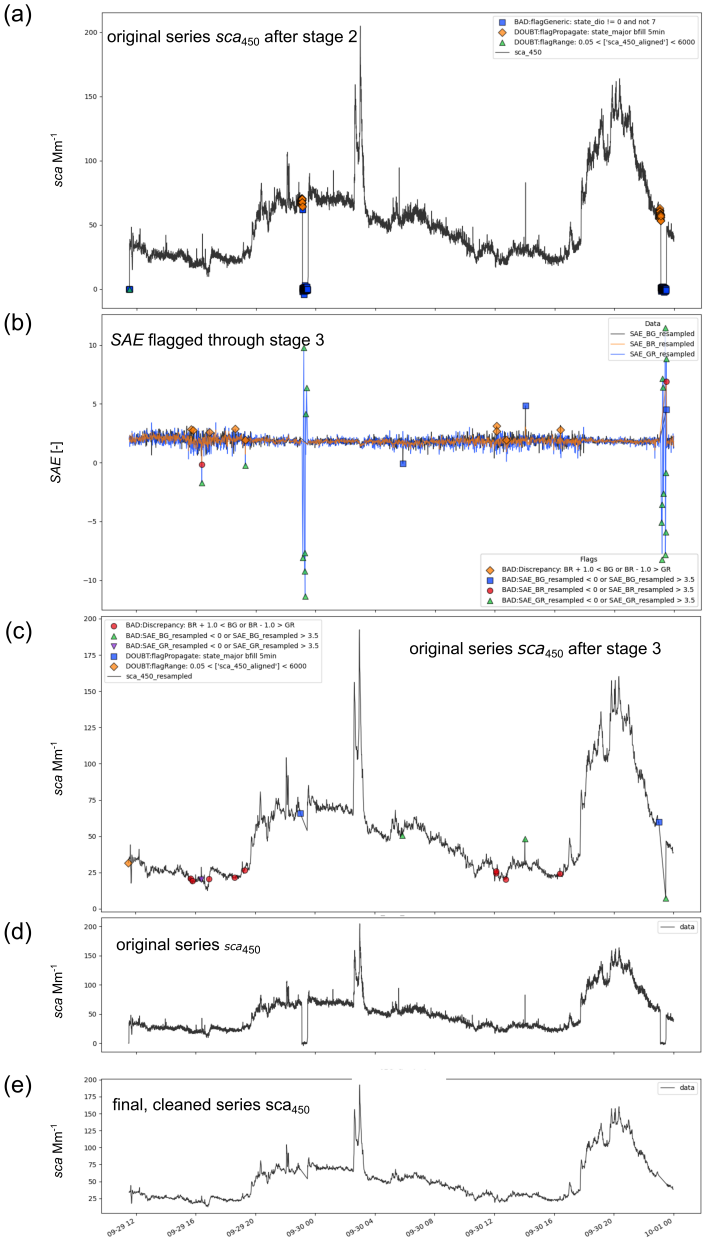

Figure 7. Resulting QC flags for `sca_450` measured by the Aurora 4000 nephelometer at the TROPOS measurement site for anomaly bc1. (a) Flags after Stage 2 (channel-level QC of `sca_450`), (b) flags from QC tests applied to the derived SAE time series (Stage 3), (c) Stage 3 flags propagated back to the final variable of interest `sca_450`, (d) original `sca_450` series, (e) final, cleaned `sca_450` series after applying the aggregated flags.

https://doi.org/10.5194/egusphere-2026-235
Preprint. Discussion started: 13 March 2026

As described in Section 5.7, the parameters of selected SaQC tests were derived through an optimisation workflow. In January 2024 (part of anomaly bc5), the Aethalometer exhibited a strongly increased signal-to-noise ratio over several days at the beginning of its operation (Fig. 8). A sudden change in this ratio occurred, and the preceding high-noise period was successfully flagged using the `flagByScatterLowpass` method during Stage 3, while subsequent data points with lower noise levels were retained as valid. During anomaly bc5, the implemented QC pipeline also flagged additional data points beyond those directly affected by the high-noise period (Fig. 8).

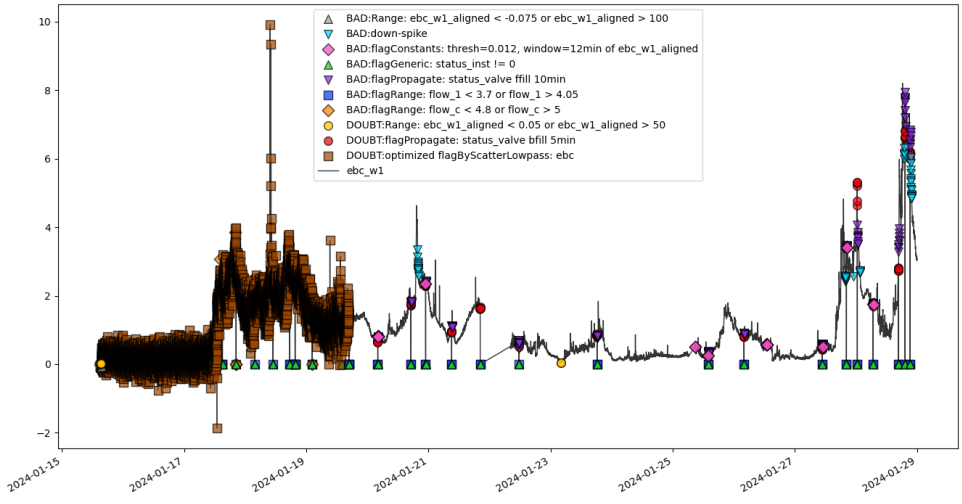

Figure 8. Equivalent black carbon `ebc_w1` from the Aethalometer at the TROPOS measurement site. Depicted is the time range corresponding to anomaly bc5, where increased channel noise was detected and consequently flagged by the QC pipeline.

6.4 Validation with Melpitz Data

Data from the Melpitz measurement site were used to validate the parameterised QC pipeline derived from the TROPOS data set. Two representative anomaly examples are shown for each instrument.

6.4.1 Aethalometer

Figure 9a shows the time range for anomaly bc5-mel and the first channel `ebc_w1` of the Aethalometer. After Stage 2, both device-control tests and channel-specific tests have triggered flags. Several downward spikes are removed based on the ranges of device-control variables and device-specific events. Preceding and subsequent data points around these events are flagged through temporal flag propagation, analogous to the TROPOS example.

The results of Stage 3 are depicted in Fig. 9b, where periods with low `ebc_w1` values are partly flagged because the corresponding AAE values fall outside the plausible range. Figure 9c illustrates the transfer of these derived-variable flags to `ebc_w1`, and Fig. 9d shows the final cleaned and resampled series, in which the anomalies of anomaly bc5-mel have been successfully removed.

https://doi.org/10.5194/egusphere-2026-235
Preprint. Discussion started: 13 March 2026

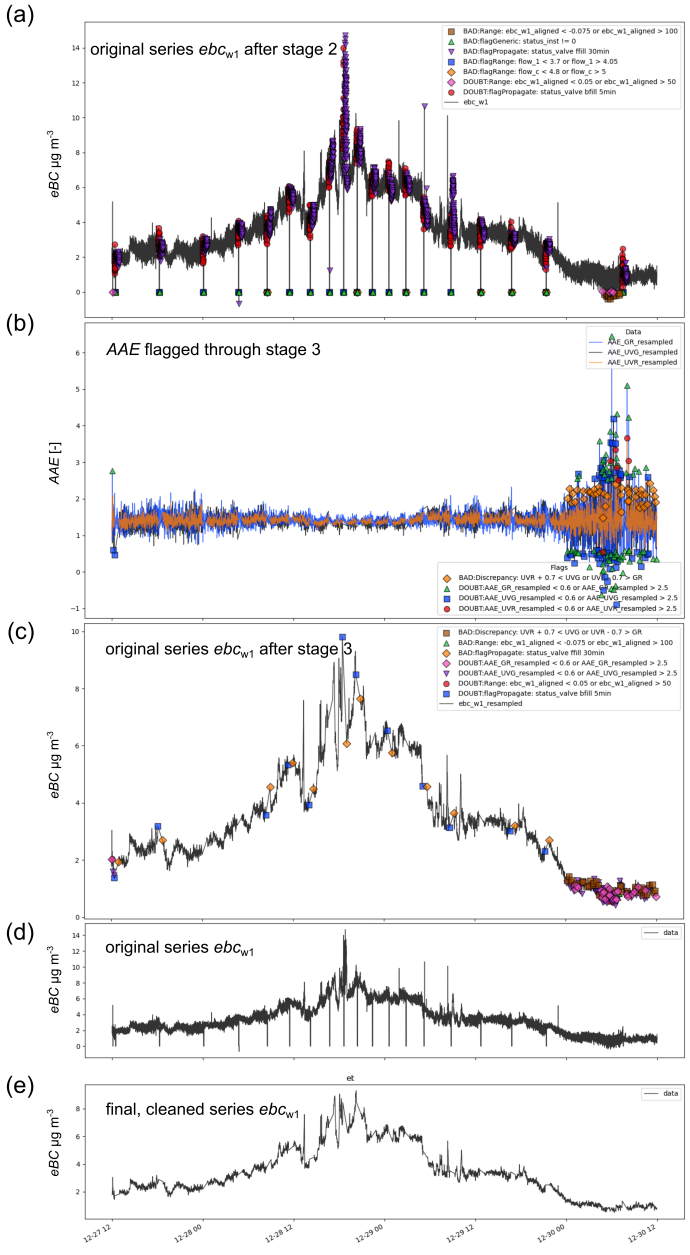

Figure 9. Resulting QC flags for `ebc_w1` measured by the AE33 Aethalometer at the Melpitz measurement site for anomaly bc5-mel. (a) Flags after Stage 2 (channel-level QC of `ebc_w1`), (b) flags from QC tests applied to the derived *AAE* time series (Stage 3), (c) Stage 3 flags propagated back to the final variable of interest `ebc_w1`, (d) original `ebc_w1` series, (e) final, cleaned `ebc_w1` series after applying the aggregated flags.

https://doi.org/10.5194/egusphere-2026-235
Preprint. Discussion started: 13 March 2026

The Melpitz data set generally shows a higher background noise level than TROPOS. As a consequence, the parameterised noise detection method (`flagByScatterLowpass`) was disabled for this site to avoid flagging large portions of the data as `DOUBTFUL`. Whether to activate this test is ultimately a station-level decision; a switch for this is provided in the user configuration (Fig. 4).

6.4.2 Nephelometer

An example of the validation of the parameterised QC workflow for the Nephelometer is shown in Fig. 10. During a period of approximately two days, several anomalies are detected by device-control variables in Stage 2 (Fig. 10a). By applying range tests to the derived SAE series (Fig. 10b), remaining implausible downward spikes and data points from very low-value periods are flagged.

6.5 Flag Statistics and Performance Indicators

QC procedures were applied to the selected anomalies with varying time-series lengths and numbers of records. For each anomaly, the flag statistics were collected and the total processing time up to the end of Stage 3, including figure creation and data export, was measured. Table 2 summarises the results for both measurement sites (TROPOS and Melpitz) and both instruments.

For the TROPOS data set and the investigated anomalies, the rule-based system flags approximately 24 % of `ebc_w1` records and 4 % of `sca_450` measurements as `DOUBTFUL` or `BAD`, while the majority of data points pass the QC pipeline without any quality flag and are thus labelled as valid (Fig. 11a). QC processing times correlate with the number of data points, although the scaling is not strictly linear due to workflow overhead (e.g. figure and file export) and the increased cost of some QC tests. The Aethalometer QC generally takes longer because more tests are implemented. For example, anomaly ls1 with about 100 000 records (approximately 1.5 months of data) requires around 187 s to pass Stage 3, whereas shorter periods such as bc1 (2 279 records, roughly two days) require about 33 s. A similar behaviour is observed for the Nephelometer workflow, with very long time series processing relatively efficiently once initial overheads are amortised.

For several anomalies in the Melpitz data set (bc1-mel, bc3-mel, bc4-mel, ls2-mel, ls3-mel), the device-control variable `status_inst` leads to flags over the entire period (red bars in Fig. 11b), so these cases are not discussed further in the preceding result subsections. For the remaining anomalies, roughly 15 % of `ebc_w1` records and 3 % of `sca_450` measurements are flagged as `DOUBTFUL` or `BAD`. The relationship between record count and processing time is weaker than for the TROPOS Aethalometer examples, but processing times remain on the order of 35 s for time series with up to about 30 000 records (approximately three days of data).

Overall, these statistics demonstrate that the automated, rule-based QC workflow can robustly handle typical anomaly patterns while keeping computational costs low enough for near-real-time operation and for the reprocessing of multi-month data segments on standard hardware.

7 Discussion

In this study, we present a fully parameterised quality control (QC) workflow for two key aerosol measurement instruments operated at ACTRIS stations, the AE33 Aethalometer and the Aurora 4000 Nephelometer. The workflow, implemented within the SaQC framework and wrapped by the `actris_qc` package, translates narrative QA/QC guidance into an explicit, executable and versioned rule set. It was tailored to meet the specific requirements of ACTRIS measurement sites, enabling a standardised, reproducible and transparent approach to data quality assurance. The pipeline follows the three-stage scheme described in Section 5.1 (Fig. 5), combining device-control checks, channel-specific evaluations and derived-variable assessments, thereby mirroring the multi-step screening recommended in existing QA/QC frameworks while expressing it in a machine-readable form. In particular, it provides a software-level realisation of the stepwise screening and flagging concepts formulated in the GAW aerosol measurement procedures, ACTRIS ECAC manuals for AE33 and Aurora 4000, and regulatory QA/QC handbooks for ambient air-quality networks (European Commission Joint Research Centre, 2011; German Environment Agency, 2016; World Meteorological Organization (WMO), 2016; Müller and Fiebig, 2020, 2021; ACTRIS CAIS-ECAC, 2026; U.S. Environmental Protection Agency, 2026).

https://doi.org/10.5194/egusphere-2026-235
Preprint. Discussion started: 13 March 2026

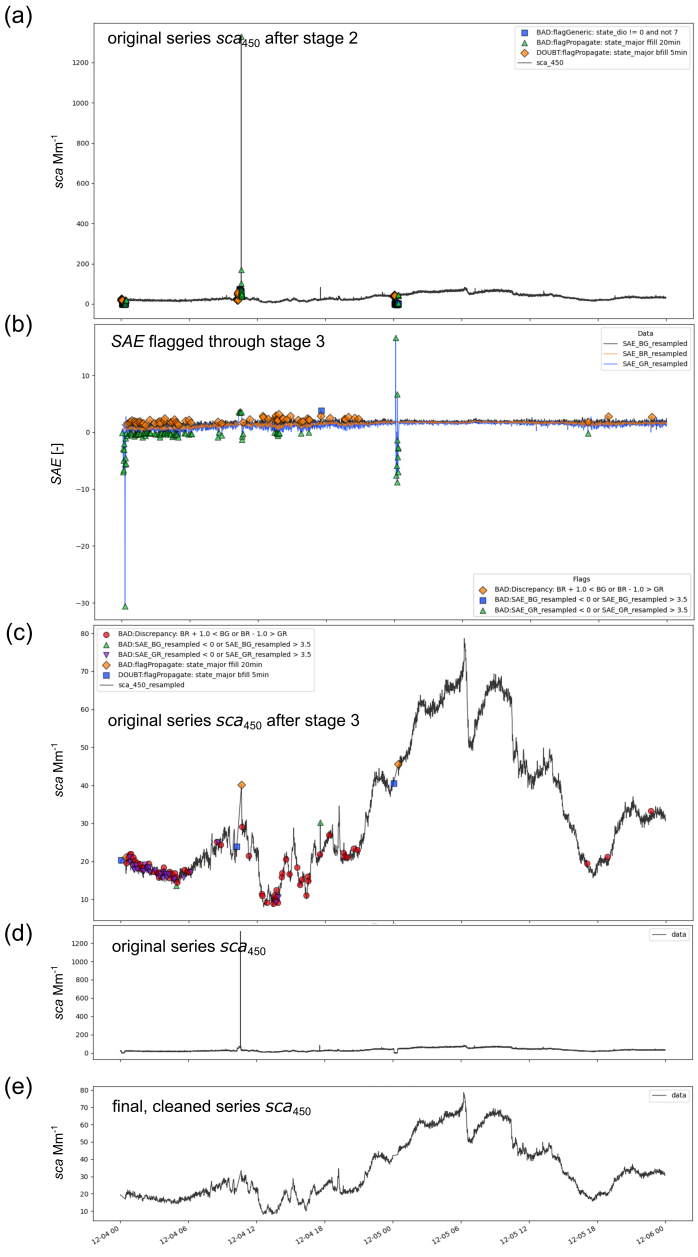

Figure 10. Resulting QC flags for `sca_450` measured by the Aurora 4000 nephelometer at the Melpitz measurement site for anomaly ls3-mel. (a) Flags after Stage 2 (channel-level QC of `sca_450`), (b) flags from QC tests applied to the derived SAE time series (Stage 3), (c) Stage 3 flags propagated back to the final variable of interest `sca_450`, (d) original `sca_450` series, (e) final, cleaned `sca_450` series after applying the aggregated flags.

https://doi.org/10.5194/egusphere-2026-235
Preprint. Discussion started: 13 March 2026

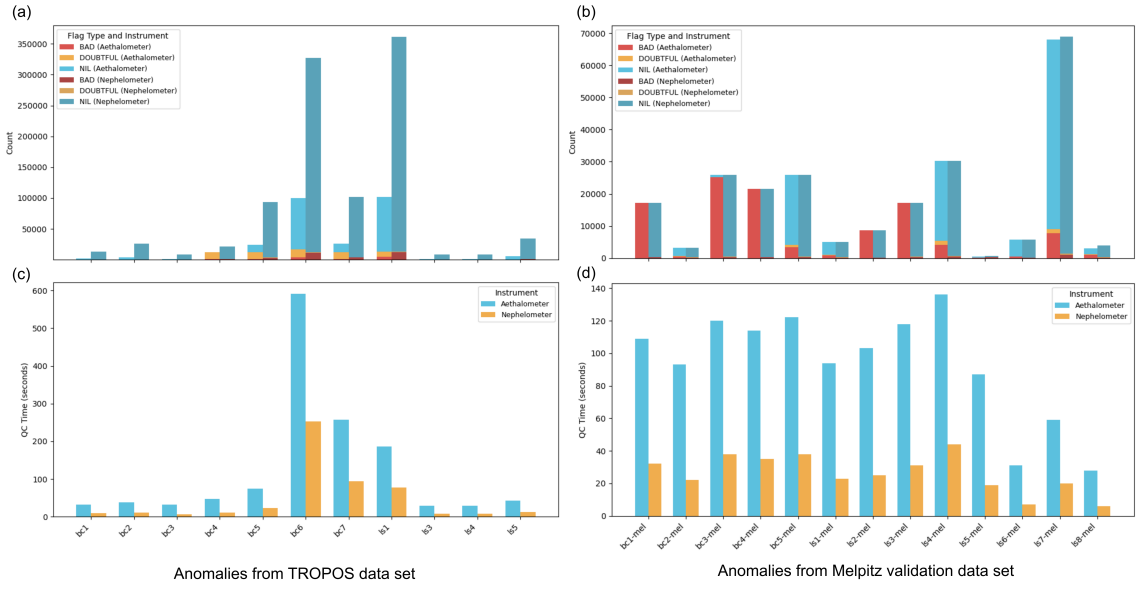

Figure 11. Flag statistics and performance indicators for selected anomalies. `NIL`: all tests passed without a flag and the record is considered `GOOD` in Table 2. (a, b) Number of data records and flag distribution for TROPOS and Melpitz, respectively; (c, d) processing time of the QC pipeline for TROPOS and Melpitz measurement sites, respectively.

Results demonstrate that manual parameterisation of the QC tests, guided by an extensive anomaly dataset from the TROPOS measurement site, is sufficient to robustly identify and flag a wide range of data irregularities. The training dataset comprised multiple anomaly types, including outliers, enhanced noise, periods of constant values and instrument-specific events. Through careful parameter tuning and sequential application of QC steps, the resulting time series were effectively cleaned, with anomalous records removed or flagged and the physical structure of genuine atmospheric variability preserved. For the TROPOS data, around 24 % of `ebc_w1` records and 4 % of `sca_450` measurements were flagged as `DOUBTFUL` or `BAD`, while the majority of data points remained unflagged and thus valid. For Melpitz, the corresponding fractions were approximately 15 % and 3 %, respectively, indicating that the workflow is neither excessively conservative nor overly permissive for the investigated datasets. Wherever possible, the Stage 1 thresholds for flow, relative humidity and device-status variables were taken directly from the above guideline documents and only refined based on the anomaly catalogue when explicit numerical recommendations were missing or too generic (European Commission Joint Research Centre, 2011; German Environment Agency, 2016; World Meteorological Organization (WMO), 2016; ACTRIS CAIS-ECAC, 2026; U.S. Environmental Protection Agency, 2026).

The cross-site transfer to the Melpitz validation dataset performed equally well, highlighting the general applicability of the parameterised workflow across different ACTRIS measurement stations with distinct environments and background noise characteristics. Only limited site-specific adjustments were necessary (e.g. deactivating the noise-detection operator for Melpitz), and these were achievable through configuration changes rather than code modifications. Together with the anomaly-based parameter optimisation (Section 5.7), this demonstrates that a single, openly documented rule set can be deployed across multiple stations and revisited when new experience accumulates.

The upper and lower bounds applied to the absorption Ångström exponents (AAE) values in this study were derived from the observations at the TROPOS and Melpitz sites. Neither dataset includes episodes of intense anthropogenic pollution or natural high-mass events such as mineral dust accumulations or wildfires, which means that the resulting value ranges reflect a combination of site-specific characteristics and the typical background aerosol regime of each station. Consequently, the limits identified here may be useful starting points for other measurement sites that do not experience extreme aerosol loading. For sites where such high-concentration events are frequent or anticipated, the bounds would need to be adjusted

https://doi.org/10.5194/egusphere-2026-235
Preprint. Discussion started: 13 March 2026

upward to avoid discarding valid data. Because the appropriate AAE thresholds are not straightforward to estimate a priori, we have explicitly determined them for the two stations under investigation. This approach highlights the need for either station-specific calibration or, preferably, a coordinated, ACTRIS-wide consensus on recommended limits.

Compared to manual data inspection, the automated QC approach offers several key advantages. Manual flagging is inherently subjective, time-consuming and difficult to reproduce, with reasoning often not systematically documented or transferable to future analyses. Controlled experiments in other domains have shown that experts can arrive at markedly different QC decisions when presented with the same dataset, even under shared guidelines. In contrast, once the SaQC workflow is parameterised, it can be applied consistently across datasets, and any subsequent adjustments (e.g. refined thresholds) can be retroactively implemented, enabling reproducible reprocessing of existing data archives. Each triggered QC test is documented with explicit labels according to the test type, allowing the entire process to be tracked and interpreted. In this sense, the workflow operationalises the responsibility for station-level data screening that GAW, ACTRIS and regulatory frameworks assign to data originators, while adding the provenance tracking and repeatability needed for FAIR data management (World Meteorological Organization (WMO), 2016; ACTRIS CAIS-ECAC, 2026; U.S. Environmental Protection Agency, 2026). This explicit provenance and flag history are particularly relevant given that purely AI-driven QC approaches, while potentially reproducible, typically lack in-depth explainability. As highlighted by Lasota et al. (2025), interpreting AI-based decisions requires extensive model evaluation and still retains a degree of uncertainty, limiting the applicability of AI alone for large-scale, high-resolution datasets without human oversight.

The initial parameterisation of SaQC for the AE33 Aethalometer and Aurora 4000 Nephelometer required substantial expert effort, especially for constructing the anomaly catalogue and tuning the most sensitive operators (e.g. noise detection). However, once established, downstream adjustments are minor and further improve workflow robustness. The generated flags and detailed annotations serve different needs and can be used to filter datasets according to specific downstream tasks. For instance, analyses may selectively consider only device-control-based flags, exclude derived-variable assessments such as absorption Ångström exponents, or combine multiple criteria, making the presented workflow adaptable for diverse scientific applications ranging from trend analysis to model evaluation.

The developed approach differs from existing complex and highly tailored methods (Giles et al., 2019; Kwon et al., 2012; Ośródka et al., 2022) in that it does not rely on multi-sensor correlation of different sources, nor on spatial correlation within dense networks of sensors of the same type as in Napoly et al. (2018); Båserud et al. (2020); Lasota et al. (2025). Furthermore, it does not perform data estimation or gap filling during the QC step, in contrast to approaches such as Wu et al. (2018). Consequently, the SaQC solution requires no external reference data or forecasts and instead focuses on the intrinsic characteristics of the individual time series. This makes the workflow comparatively straightforward to parameterise and apply, reduces the number of required assumptions and external dependencies, and helps to avoid misclassifying genuine atmospheric events (e.g. fireworks, pollution episodes, dust events) as artefacts simply because they deviate from climatological baselines or spatial patterns.

At the same time, the SaQC implementation should be viewed as a preliminary and complementary step in the broader QA/QC chain rather than as a replacement for all other procedures, in line with the multi-stage QA/QC concepts formulated in GAW, ACTRIS and regulatory guidance documents (European Commission Joint Research Centre, 2011; German Environment Agency, 2016; World Meteorological Organization (WMO), 2016; ACTRIS CAIS-ECAC, 2026; U.S. Environmental Protection Agency, 2026). It operates on level-0/1 time series prior to advanced correction or modelling steps, such as multiple-scattering and loading corrections for absorption photometers, truncation and humidity corrections for nephelometers, or source apportionment analyses, as summarised for black carbon and aerosol optics in Petzold et al. (2013); Laj et al. (2020); Savadkoohi et al. (2023, 2024); RI-URBANS (2024). The workflow ensures that obvious artefacts, instrument malfunctions and inconsistent derived parameters are flagged in a reproducible manner, thereby providing a clean and well-documented basis for subsequent harmonisation and higher-level data products. In practice, manual review and expert judgement remain essential for borderline cases, for rare or previously unseen anomaly patterns, and for evaluating long-term drifts that may be subtle on hourly time scales but significant over years.

An important added value of the presented workflow is its role in preparing data for artificial intelligence and digital-twin applications. By ensuring baseline data quality and providing labelled QC flags with explicit provenance, the workflow produces datasets that can be reliably used for tasks such as gap filling, interpolation, or training machine-learning models on regularly spaced grids. The anomaly catalogue and associated flags can themselves serve as training or validation data for future ML-based QC algorithms, including graph neural network approaches for multivariate sensor networks (Lasota

https://doi.org/10.5194/egusphere-2026-235
Preprint. Discussion started: 13 March 2026

et al., 2025). This capability significantly accelerates scientific analyses by allowing researchers to focus on data interpretation and model development rather than on preliminary quality assessments, and it helps to mitigate the risk that AI models inadvertently learn from biased or contaminated training data.

Several limitations of the present work point to avenues for further development. First, parameterisation was carried out using anomalies from two instruments and two sites; extending the workflow to a broader range of ACTRIS stations, climatic regimes and operational practices will likely reveal additional edge cases and may motivate more adaptive or context-aware thresholds. Second, only AE33 and Aurora 4000 instruments were considered. Extending the `actris_qc` package to additional devices (e.g. other absorption photometers, CAPS extinction monitors, or regulatory PM analysers) will test the generality of the rule set and of the flagging concept. Third, the current workflow focuses on short- to medium-term anomalies; systematic multi-year drift and fouling are only indirectly addressed through derived variables and will require dedicated long-term diagnostics in future work. Finally, while the anomaly-based parameter optimisation provides a pragmatic way to align automated rules with expert judgement, it also inherits any biases present in the manually flagged training data; this should be kept in mind when re-using the labelled anomalies as ground truth for ML applications.

Despite these limitations, the presented workflow already fulfils key requirements for operational use in research infrastructures. Computational performance is sufficient for near-real-time application: for example, a 1.5-month Aethalometer segment with roughly 10^5 records can be processed through all QC stages in about two to three minutes on standard hardware, while typical multi-day segments require only a few tens of seconds. The modular structure of the Python package, based on standard SaQC workflows for time series data, allows for easy extension, parameter adjustment and integration of additional devices. Once embedded into routine station operation (e.g. via scheduled execution of `run.py`), high-resolution data with a 10 s sampling interval can be screened daily with minimal operator intervention.

Overall, the QC workflow developed here establishes a reproducible, interpretable and efficient foundation for high-quality aerosol measurements in ACTRIS and beyond. By providing an open, rule-based and FAIR-compliant pipeline that operationalises existing QA/QC guidance, it offers a concrete path towards harmonised, real-time quality assurance for aerosol optical time series and thereby supports AI-ready data streams for downstream applications such as environmental digital twins and decision-support systems.

8 Conclusions

This study presents, to our knowledge, the first openly documented, fully automated and real-time-capable quality control (QC) workflow for time series from AE33 Aethalometers and Aurora 4000 nephelometers operated at ACTRIS stations. Building on the generic SaQC framework (Section 4.1) and implemented via the ACTRIS-specific `actris_qc` Python package (Section 4.2), the workflow translates narrative QA/QC guidance from ACTRIS, GAW and regulatory frameworks into an explicit, executable and versioned rule set. It is tailored to ACTRIS station operation but remains sufficiently generic to be transferred to other networks and instruments.

Following the three-stage pipeline described in Section 5.1 (Fig. 5), using an anomaly catalogue compiled from two years of TROPOS urban data, we manually tuned and optimised the SaQC operators so that the workflow robustly identifies typical artefacts – including outliers, enhanced noise, plateaus, implausible ranges and device events – while preserving genuine atmospheric variability. Application to the independent Melpitz dataset shows that the same configuration can be transferred across stations with only minor, configuration-level adaptations, confirming its robustness under different environmental and noise conditions.

For the selected anomaly periods, approximately 24 % of Aethalometer records and 4 % of nephelometer measurements at TROPOS, and 15 % and 3 %, respectively, at Melpitz were flagged as `DOUBTFUL` or `BAD`, while the majority of data points remained unflagged and thus valid. Computational performance is sufficient for near-real-time operation: multi-week segments with $\mathcal{O}(10^5)$ records can be processed through all QC stages in a few minutes on standard hardware, and typical multi-day windows require only a few tens of seconds. This makes it feasible to run the workflow operationally at ACTRIS stations and to reprocess historical archives under updated configurations.

Beyond its performance, the workflow offers several qualitative advantages. It provides an objective, rule-based alternative to manual inspection, with every QC decision traceable to specific tests and parameters. Once parameterised, the same rule

https://doi.org/10.5194/egusphere-2026-235
Preprint. Discussion started: 13 March 2026

set can be applied consistently across datasets, and subsequent adjustments can be propagated retrospectively, ensuring reproducible and transparent reprocessing. The modular design of `actris_qc`, which separates generic SaQC operators from instrument-specific configurations and data-access routines, facilitates extension to additional devices and networks with limited additional implementation effort. By integrating device-specific rules and derived diagnostics such as AAE and SAE into a single framework, the workflow captures both direct and more subtle anomalies without relying on external reference data or complex multi-sensor constellations.

A further outcome of this work is the generation of labelled, AI-ready datasets. The QC flags and their explicit provenance can be used directly for resampling, filtering and uncertainty-aware analyses, and they provide training and validation data for future machine-learning-based QC approaches, including graph-based methods for multivariate sensor networks. In this way, the workflow not only stabilises current operational data streams but also prepares the ground for advanced applications such as gap filling, data assimilation and environmental digital twins.

At the same time, the presented solution is not intended to replace existing QA/QC practices but to complement them as a standardised first step on level-0/1 time series. It delivers a clean and well-documented basis for subsequent instrument-specific corrections, long-term consistency checks, source apportionment and network-wide analyses, and it makes the station-level responsibility for data screening operational in a reproducible way. Future work will focus on extending `actris_qc` to additional instruments (e.g. other absorption photometers, extinction instruments and regulatory PM analysers), broadening the anomaly catalogue across more ACTRIS sites and climatic regimes, and exploring hybrid schemes in which rule-based QC and interpretable machine-learning methods jointly address complex or previously unseen anomaly patterns.

Overall, the QC workflow developed here establishes a reproducible, interpretable and efficient foundation for high-quality aerosol measurements in ACTRIS and beyond. By providing an open, rule-based and FAIR-aligned pipeline that operationalises existing QA/QC guidance, it offers a concrete path towards harmonised, real-time quality assurance for aerosol optical time series and towards robust, AI-ready data streams for the next generation of atmospheric research and decision-support systems.

Code and data availability. The Python package `actris_qc` is hosted on Helmholtz GitLab (`https://codebase.helmholtz.cloud/qc-of-atmospheric-time-series/actris-quality-control`) and is archived on Zenodo (Houben et al., 2026b). The data sets and associated quality-control outputs presented in this work, including flags (CSV), logs (TXT) and diagnostic figures (PNG), are available via Zenodo (Houben et al., 2026a).

Appendix A: Summary of QC parameterization

Appendix B: Estimation of Filter Loading Effect

Author contributions. Conceptualization: TH, TM, JB, Data curation: TH, TM, JV, Formal analysis: TH, PL, Funding acquisition: JB, Investigation: TH, PL, Methodology: TH, TM, JB, Project administration: TT, Resources: TM, JV, Software: DS, Supervision: JB, Validation: TH, Visualization: TH, Writing (original draft preparation): TH, JB, JV, EV, TT

Competing interests. The authors declare no competing interests.

Acknowledgements. The research is part of the project Artificial Intelligence and Mobility (AIAMO), funded by the German Federal Ministry for Digital and Transport (BMDV) under Founding 45KI19D041 (BMVI BAV).

We thank the Helmholtz Association, Germany and the Federal Ministry of Research, Technology and Space (BMFTR), Germany through the Helmholtz DataHub initiative of the Research Field Earth and Environment, and by the Helmholtz Earth and Environment Program ‘Changing Earth — Sustaining our Future’. The DataHub enables overarching and comprehensive research data management, in accordance with the FAIR principles, for all topics of the Earth and Environment programme.

https://doi.org/10.5194/egusphere-2026-235
Preprint. Discussion started: 13 March 2026

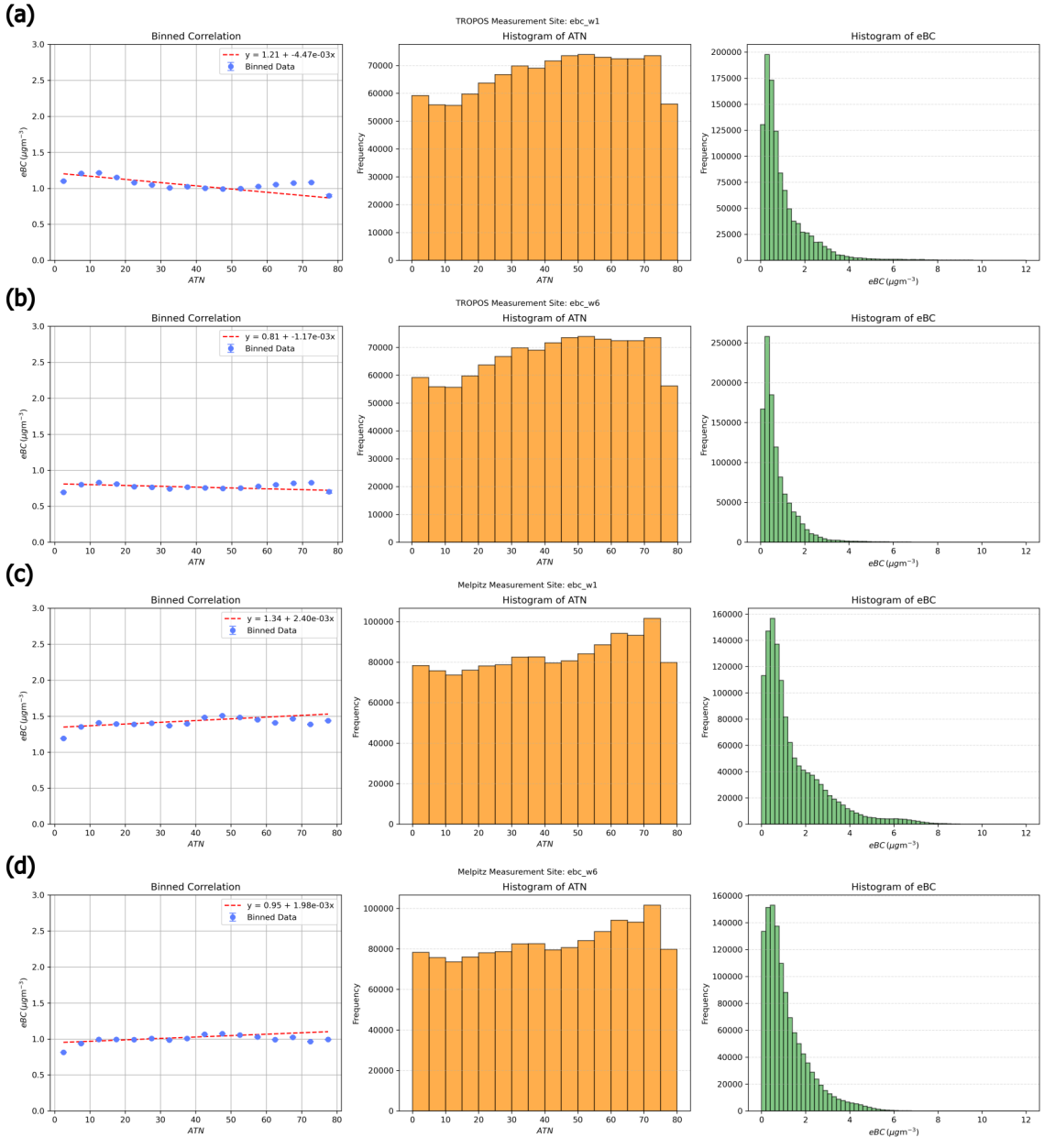

Figure B1. left: Binned correlation of equivalent black carbon eBC of the first channel and attenuation of spot 1 including error of standard deviation for each bin, mid: Histogram of attenuation values, right: Histogram of eBC values. (a) TROPOS measurement site for ebc of first channel, (b) TROPOS measurement site for ebc of sixth channel, (c) Melpitz measurement site for ebc of first channel, (d) Melpitz measurement site for ebc of sixth channel.

The scientific results have been computed at the High-Performance Computing (HPC) Cluster EVE, a joint effort of both the Helmholtz Centre for Environmental Research - UFZ and the German Centre for Integrative Biodiversity Research (iDiv) Halle-Jena-Leipzig.

https://doi.org/10.5194/egusphere-2026-235
Preprint. Discussion started: 13 March 2026

Parts of the python code has been generated by large language models (LLM) via prompts and was further manually adapted and checked. The language of the manuscript was partially improved using LLMs, however, no content generated by these tools was incorporated without careful review and verification.

References

ACTRIS-2 Consortium: WP4 Deliverable D4.1: Progress report on standard-making process., Tech. rep., https://actris.eu/sites/default/files/Documents/ACTRIS-2/Deliverables/WP4_D4.1_M22.pdf, 2017a.

ACTRIS-2 Consortium: WP3 Deliverable D3.11: Reference instruments for multi-wavelength absorptionmeasurements, Tech. rep., https://www.actris.eu/sites/default/files/Documents/ACTRIS-2/Deliverables/WP3_D3.11_M28.pdf, 2017b.

ACTRIS-2 Consortium: WP11 Deliverable D11.4: Report on closure results between the measurements ofabsorption coefficient and black carbon concentration, Tech. rep., https://actris.eu/sites/default/files/Documents/ACTRIS-2/Deliverables/WP11_D11.4_M42.pdf, 2018.

ACTRIS-2 Consortium: WP9 Deliverable D 9.2: Final report on access to advanced ACTRIS stations, Tech. rep., https://actris.eu/sites/default/files/Documents/ACTRIS-2/Deliverables/WP9_D9.2_M48_vf.pdf, 2019.

ACTRIS CAIS-ECAC: Measurement Guidelines for Aerosol In-situ Measurements, https://www.actris-ecac.eu/measurement-guidelines.html, Accessed: 2026-01-02, 2026.

Anderson, T., Covert, D., Marshall, S., Laucks, M., Charlson, R., Waggoner, A., Ogren, J., Caldow, R., Holm, R., Quant, F., Sem, G., Wiedensohler, A., Ahlquist, N., and Bates, T.: Performance Characteristics of a High-Sensitivity, Three-Wavelength, Total Scatter/Backscatter Nephelometer, Journal of Atmospheric and Oceanic Technology, 13, 967–986, https://doi.org/10.1175/1520-0426(1996)013<0967:PCOAHS>2.0.CO;2, 1996.

Andrews, E., Sheridan, P. J., Ogren, J. A., Hageman, D., Jefferson, A., Wendell, J., et al.: Overview of the NOAA/ESRL Federated Aerosol Network, Bulletin of the American Meteorological Society, 100, 123–135, https://doi.org/10.1175/BAMS-D-17-0175.1, 2019.

Asmi, E., Backman, J., Servomaa, H., Virkkula, A., Gini, M. I., Eleftheriadis, K., Müller, T., Ohata, S., Kondo, Y., and Hyvärinen, A.: Absorption instruments inter-comparison campaign at the Arctic Pallas station, Atmospheric Measurement Techniques, 14, 5397–5413, https://doi.org/10.5194/amt-14-5397-2021, 2021.

Bagkis, E., Kassandros, T., and Karatzas, K.: Learning Calibration Functions on the Fly: Hybrid Batch Online Stacking Ensembles for the Calibration of Low-Cost Air Quality Sensor Networks in the Presence of Concept Drift, Atmosphere, 13, https://doi.org/10.3390/atmos13030416, 2022.

Bagkis, E., Hassani, A., Schneider, P., DeSouza, P., Shetty, S., Kassandros, T., Salamalikis, V., Castell, N., Karatzas, K., Ahlawat, A., and Khan, J.: Evolving trends in application of low-cost air quality sensor networks: challenges and future directions, npj Climate and Atmospheric Science, 8, 335, https://doi.org/10.1038/s41612-025-01216-4, 2025.

Bauer, P., Dueben, P. D., Hoefler, T., Quintino, T., Schulthess, T. C., and Wedi, N. P.: The digital revolution of Earth-system science, Nature Computational Science, 1, 104–113, https://doi.org/10.1038/s43588-021-00023-0, 2021a.

Bauer, P., Stevens, B., and Hazeleger, W.: A digital twin of Earth for the green transition, Nature Climate Change, 11, 80–83, https://doi.org/10.1038/s41558-021-00986-y, 2021b.

Beck, I., Angot, H., Baccarini, A., Dada, L., Quéléver, L., Jokinen, T., Laurila, T., Lampimäki, M., Bukowiecki, N., Boyer, M., Gong, X., Gysel-Beer, M., Petäjä, T., Wang, J., and Schmale, J.: Automated identification of local contamination in remote atmospheric composition time series, Atmospheric Measurement Techniques, 15, 4195–4224, https://doi.org/10.5194/amt-15-4195-2022, 2022.

Bumberger, J., Abbrent, M., Brinckmann, N., Hemmen, J., Kunkel, R., Lorenz, C., Lünenschloss, P., Palm, B., Schnicke, T., Schulz, C., Van Der Schaaf, H., and Schäfer, D.: Digital ecosystem for FAIR time series data management in environmental system science, SoftwareX, 29, 102 038, https://doi.org/10.1016/j.softx.2025.102038, 2025.

Båserud, L., Lussana, C., Nipen, T. N., Seierstad, I. A., Oram, L., and Aspelien, T.: TITAN automatic spatial quality control of meteorological in-situ observations, Advances in Science and Research, 17, 153–163, https://doi.org/10.5194/asr-17-153-2020, 2020.

Calvin, K., Dasgupta, D., Krinner, G., Mukherji, A., Thorne, P. W., Trisos, C., Romero, J., Aldunce, P., Barrett, K., Blanco, G., Cheung, W. W., Connors, S., Denton, F., Diongue-Niang, A., Dodman, D., Garschagen, M., Geden, O., Hayward, B., Jones, C., Jotzo, F., Krug, T., Lasco, R., Lee, Y.-Y., Masson-Delmotte, V., Meinshausen, M., Mintenbeck, K., Mokssit, A., Otto, F. E., Pathak, M., Pirani, A., Poloczanska, E., Pörtner, H.-O., Revi, A., Roberts, D. C., Roy, J., Ruane, A. C., Skea, J., Shukla, P. R., Slade, R., Slangen, A., Sokona, Y., Sörensson, A. A., Tignor, M., Van Vuuren, D., Wei, Y.-M., Winkler, H., Zhai, P., Zommers, Z., Hourcade, J.-C., Johnson, F. X., Pachauri, S., Simpson, N. P., Singh, C., Thomas, A., Totin, E., Alegría, A., Armour, K., Bednar-Friedl, B., Blok, K., Cissé, G., Dentener, F., Eriksen, S., Fischer, E., Garner, G., Guivarch, C., Haasnoot, M., Hansen, G., Hauser, M., Hawkins, E., Hermans, T., Kopp, R., Leprince-Ringuet, N., Lewis, J., Ley, D., Ludden, C., Niamir, L., Nicholls, Z., Some, S., Szopa, S., Trewin, B., Van Der Wijst, K.-I., Winter, G., Witting, M., Birt, A., Ha, M., Arias, P., Bustamante, M., Elgizouli, I., Flato, G., Howden, M., Méndez-Vallejo, C., Pereira, J. J., Pichs-Madruga, R., Rose, S. K., Saheb, Y., Sánchez Rodríguez, R., Ürge Vorsatz, D., Xiao, C., Yassaa, N., Romero, J., Kim, J., Haites, E. F., Jung, Y., Stavins, R., Birt, A., Ha, M., Orendain, D. J. A., Ignon, L., Park, S., Park, Y., Reisinger, A., Cammaramo, D., Fischlin, A., Fuglestvedt, J. S., Hansen, G., Ludden, C., Masson-Delmotte, V., Matthews, J. R., Mintenbeck, K., Pirani, A., Poloczanska, E., Leprince-Ringuet, N., and Péan, C.: Synthesis Report. Contribution of Working Groups I, II and III to the Sixth Assessment Report of the Intergovernmental Panel on Climate Change, Tech. rep., Intergovernmental Panel on Climate Change (IPCC), https://doi.org/10.59327/ipcc/ar6-9789291691647, 2023.

https://doi.org/10.5194/egusphere-2026-235
Preprint. Discussion started: 13 March 2026

Campbell, J. L., Rustad, L. E., Porter, J. H., Taylor, J. R., Dereszynski, E. W., Shanley, J. B., Gries, C., Henshaw, D. L., Martin, M. E., Sheldon, W. M., and Boose, E. R.: Quantity is Nothing without Quality: Automated QA/QC for Streaming Environmental Sensor Data, BioScience, 63, 574–585, https://doi.org/10.1525/bio.2013.63.7.10, 2013.

Carotenuto, F., Bisignano, A., Brilli, L., Gualtieri, G., and Giovannini, L.: Low-cost air quality monitoring networks for long-term field campaigns: A review, Meteorological Applications, 30, e2161, https://doi.org/https://doi.org/10.1002/met.2161, 2023.

Chabbi, A. and Loescher, H. W., eds.: Terrestrial Ecosystem Research Infrastructures: Challenges and Opportunities, CRC Press, Boca Raton, https://doi.org/10.1201/9781315368252, 2017.

Chu, H.-J., Ali, M. Z., and He, Y.-C.: Spatial calibration and PM2.5 mapping of low-cost air quality sensors, Scientific Reports, 10, 22 079, https://doi.org/10.1038/s41598-020-79064-w, 2020.

Clouse, S.: Air Monitoring Documentation, Data Review, and Validation Procedure, Procedure Publication 17-02-013, Olympia, Washington, https://apps.ecology.wa.gov/publications/documents/1702013.pdf, 2024.

Cuesta-Mosquera, A., Močnik, G., Drinovec, L., Müller, T., Pfeifer, S., Minguillón, M. C., Briel, B., Buckley, P., Dudoitis, V., Fernández-García, J., Fernández-Amado, M., Ferreira De Brito, J., Riffault, V., Flentje, H., Heffernan, E., Kalivitis, N., Kalogridis, A.-C., Keernik, H., Marmureanu, L., Luoma, K., Marinoni, A., Pikridas, M., Schauer, G., Serfozo, N., Servomaa, H., Titos, G., Yus-Díez, J., Zioła, N., and Wiedensohler, A.: Intercomparison and characterization of 23 Aethalometers under laboratory and ambient air conditions: procedures and unit-to-unit variabilities, Atmospheric Measurement Techniques, 14, 3195–3216, https://doi.org/https://doi.org/10.5194/amt-8-1965-2015, 2021.

Drinovec, L., Močnik, G., Zotter, P., Prévôt, A. S. H., Ruckstuhl, C., Coz, E., Rupakheti, M., Sciare, J., Müller, T., Wiedensohler, A., and Hansen, A. D. A.: The "dual-spot" Aethalometer: an improved measurement of aerosol black carbon with real-time loading compensation, Atmospheric Measurement Techniques, 8, 1965–1979, https://doi.org/10.5194/amt-8-1965-2015, 2015.

European Commission Joint Research Centre: A Quality Assurance and Control Program for PM2.5 and PM10 Measurements in European Air Quality Monitoring Networks, Tech. Rep. EUR 24851 EN, https://doi.org/10.2788/31647, 2011.

European Environment Agency and European Commission Joint Research Centre: The application of models under the European Union's Air Quality Directive: A technical reference guide, Tech. Rep. 10, https://doi.org/10.2800/80600, 2011.

European Metrology Network for Pollution Monitoring: Standardisation of Black Carbon aerosol metrics for air quality and climate modelling (STANBC, Project 22NRM02), https://www.euramet.org/european-metrology-networks/pollution-monitoring/activities-impact/projects/details/project/standardisation-of-black-carbon-aerosol-metrics-for-air-quality-and-climate-modelling, accessed 2026-03-11, 2026.

European Parliament and Council of the European Union: Directive (EU) 2024/2881 of the European Parliament and of the Council of 23 October 2024 on ambient air quality and cleaner air for Europe (recast), Official Journal of the European Union, L 2024/2881, https://eur-lex.europa.eu/eli/dir/2024/2881/oj/eng, 2024.

Ferrero, L., Losi, N., Rigler, M., Gregorič, A., Colombi, C., D'Angelo, L., Cuccia, E., Cefalì, A., Gini, I., Doldi, A., Cerri, S., Maroni, P., Cipriano, D., Markuszewski, P., and Bolzacchini, E.: Determining the Aethalometer multiple scattering enhancement factor C from the filter loading parameter, Science of The Total Environment, 917, 170 221, https://doi.org/10.1016/j.scitotenv.2024.170221, 2024.

Gäbel, P. and Hertig, E.: Recalibration of low-cost air pollution sensors: Is it worth it?, EGUsphere, 2025, 1–39, https://doi.org/10.5194/egusphere-2025-2677, 2025.

German Environment Agency: Guideline on Air Quality Plans, Brochur, ISSN 2363-832X, https://www.umweltbundesamt.de/sites/default/files/medien/1410/publikationen/broschuere_guideline_airqualityplans_en.pdf, 2016.

Giles, D. M., Sinyuk, A., Sorokin, M. G., Schafer, J. S., Smirnov, A., Slutsker, I., Eck, T. F., Holben, B. N., Lewis, J. R., Campbell, J. R., Welton, E. J., Korkin, S. V., and Lyapustin, A. I.: Advancements in the Aerosol Robotic Network (AERONET) Version 3 database – automated near-real-time quality control algorithm with improved cloud screening for Sun photometer aerosol optical depth (AOD) measurements, Atmospheric Measurement Techniques, 12, 169–209, https://doi.org/10.5194/amt-12-169-2019, 2019.

Gualtieri, G., Ahbil, K., Brilli, L., Carotenuto, F., Cavaliere, A., Gioli, B., Giordano, T., Katiellou, G. L., Mouhaimini, M., Tarchiani, V., Vagnoli, C., Zaldei, A., and Bacci, M.: Potential of low-cost PM monitoring sensors to fill monitoring gaps in areas of Sub-Saharan Africa, Atmospheric Pollution Research, 15, 102 158, https://doi.org/10.1016/j.apr.2024.102158, 2024.

Hayward, I., Martin, N. A., Ferracci, V., Kazemimanesh, M., and Kumar, P.: Low-Cost Air Quality Sensors: Biases, Corrections and Challenges in Their Comparability, Atmosphere, 15, https://doi.org/10.3390/atmos15121523, 2024.

Hazeleger, W., Aerts, J. P. M., Bauer, P., Bierkens, M. F. P., Camps-Valls, G., Dekker, M. M., Doblas-Reyes, F. J., Eyring, V., Finkenauer, C., Grundner, A., Hachinger, S., Hall, D. M., Hartmann, T., Iglesias-Suarez, F., Janssens, M., Jones, E. R., Kölling, T., Lees, M., Lhermitte, S., van Nieuwpoort, R. V., Pahker, A.-K., Pellicer-Valero, O. J., Pijpers, F. P., Siibak, A., Spitzer, J., Stevens, B., Vasconcelos, V. V., and Vossepoel, F. C.: Digital twins of the Earth with and for humans, Communications Earth & Environment, 5, 463, https://doi.org/10.1038/s43247-024-01626-x, 2024.

Heiskanen, J., Brümmer, C., Buchmann, N., Calfapietra, C., Chen, H., Gielen, B., Gkritzalis, T., Hammer, S., Hartman, S., Herbst, M., Janssens, I. A., Jordan, A., Juurola, E., Karstens, U., Kasurinen, V., Kruijt, B., Lankreijer, H., Levin, I., Linderson, M.-L., Loustau, D., Merbold, L., Myhre, C. L., Papale, D., Pavelka, M., Pilegaard, K., Ramonet, M., Rebmann, C., Rinne, J., Rivier, L., Saltikoff, E., Sanders, R., Steinbacher, M., Steinhoff, T., Watson, A., Vermeulen, A. T., Vesala, T., Vítková, G., and Kutsch, W.: The Integrated Carbon Observation System in Europe, Bulletin of the American Meteorological Society, 103, E855–E872, https://doi.org/10.1175/bams-d-19-0364.1, 2022.

https://doi.org/10.5194/egusphere-2026-235
Preprint. Discussion started: 13 March 2026

Houben, T., Müller, T., Lünenschloß, P., Voigtländer, J., Trabert, T., Vosgerau, E., Schäfer, D., and Bumberger, J.: Real-time automated quality control of atmospheric aerosol time series, https://doi.org/10.5281/ZENODO.18234702, 2026a.

Houben, T., Müller, T., Lünenschloß, P., Voigtländer, J., Trabert, T., Vosgerau, E., Schäfer, D., and Bumberger, J.: Real-time automated quality control of atmospheric aerosol time series, https://doi.org/10.5281/ZENODO.18234957, 2026b.

Jones, A. S., Horsburgh, J. S., and Eiriksson, D. P.: Assessing subjectivity in environmental sensor data post processing via a controlled experiment, Ecological Informatics, 46, 86–96, https://doi.org/10.1016/j.ecoinf.2018.05.001, 2018.

Kaffashzadeh, N., Kleinert, F., and Schultz, M. G.: A New Tool for Automated Quality Control of Environmental Time Series (AutoQC4Env) in Open Web Services, in: Business Information Systems Workshops, edited by Abramowicz, W. and Corchuelo, R., pp. 513–518, Springer International Publishing, Cham, https://doi.org/10.1007/978-3-030-36691-9_43, 2019.

Khedr, M., Liu, X., Hadiatullah, H., Orasche, J., Zhang, X., Cyrys, J., Michalke, B., Zimmermann, R., and Schnelle-Kreis, J.: Influence of New Year's fireworks on air quality – A case study from 2010 to 2021 in Augsburg, Germany, Atmospheric Pollution Research, 13, 101 341, https://doi.org/10.1016/j.apr.2022.101341, 2022.

Kwon, E.-H., Li, J., Li, J., Sohn, B. J., and Weisz, E.: Use of total precipitable water classification of a priori error and quality control in atmospheric temperature and water vapor sounding retrieval, Advances in Atmospheric Sciences, 29, 263–273, https://doi.org/10.1007/s00376-011-1119-z, 2012.

Laj, P., Bigi, A., Rose, C., Andrews, E., Lund Myhre, C., Collaud Coen, M., Lin, Y., Wiedensohler, A., Schulz, M., Ogren, J. A., Fiebig, M., Gliß, J., Mortier, A., Pandolfi, M., Petäja, T., Kim, S.-W., Aas, W., Putaud, J.-P., Mayol-Bracero, O., Keywood, M., Labrador, L., Aalto, P., Ahlberg, E., Alados Arboledas, L., Alastuey, A., Andrade, M., Artíñano, B., Ausmeel, S., Arsov, T., Asmi, E., Backman, J., Baltensperger, U., Bastian, S., Bath, O., Beukes, J. P., Brem, B. T., Bukowiecki, N., Conil, S., Couret, C., Day, D., Dayantolis, W., Degorska, A., Eleftheriadis, K., Fetfatzis, P., Favez, O., Flentje, H., Gini, M. I., Gregorič, A., Gysel-Beer, M., Hallar, A. G., Hand, J., Hoffer, A., Hueglin, C., Hooda, R. K., Hyvärinen, A., Kalapov, I., Kalivitis, N., Kasper-Giebl, A., Kim, J. E., Kouvarakis, G., Kranjc, I., Krejci, R., Kulmala, M., Labuschagne, C., Lee, H.-J., Lihavainen, H., Lin, N.-H., Löschau, G., Luoma, K., Marinoni, A., Martins Dos Santos, S., Meinhardt, F., Merkel, M., Metzger, J.-M., Mihalopoulos, N., Nguyen, N. A., Ondracek, J., Pérez, N., Perrone, M. R., Petit, J.-E., Picard, D., Pichon, J.-M., Pont, V., Prats, N., Prenni, A., Reisen, F., Romano, S., Sellegri, K., Sharma, S., Schauer, G., Sheridan, P., Sherman, J. P., Schütze, M., Schwerin, A., Sohmer, R., Sorribas, M., Steinbacher, M., Sun, J., Titos, G., Toczko, B., Tuch, T., Tulet, P., Tunved, P., Vakkari, V., Velarde, F., Velasquez, P., Villani, P., Vratolis, S., Wang, S.-H., Weinhold, K., Weller, R., Yela, M., Yus-Diez, J., Zdimal, V., Zieger, P., and Zikova, N.: A global analysis of climate-relevant aerosol properties retrieved from the network of Global Atmosphere Watch (GAW) near-surface observatories, Atmospheric Measurement Techniques, 13, 4353–4392, https://doi.org/10.5194/amt-13-4353-2020, 2020.

Laj, P., Lund Myhre, C., Riffault, V., Amiridis, V., Fuchs, H., Eleftheriadis, K., Petäjä, T., Salameh, T., Kivekäs, N., Juurola, E., Saponaro, G., Philippin, S., Cornacchia, C., Alados Arboledas, L., Baars, H., Claude, A., De Mazière, M., Dils, B., Dufresne, M., Evangeliou, N., Favez, O., Fiebig, M., Haeffelin, M., Herrmann, H., Höhler, K., Illmann, N., Kreuter, A., Ludewig, E., Marinou, E., Möhler, O., Mona, L., Eder Murberg, L., Nicolae, D., Novelli, A., O'Connor, E., Ohneiser, K., Petracca Altieri, R. M., Picquet-Varrault, B., Van Pinxteren, D., Pospichal, B., Putaud, J.-P., Reimann, S., Siomos, N., Stachlewska, I., Tillmann, R., Voudouri, K. A., Wandinger, U., Wiedensohler, A., Apituley, A., Comerón, A., Gysel-Beer, M., Mihalopoulos, N., Nikolova, N., Pietruczuk, A., Sauvage, S., Sciare, J., Skov, H., Svendby, T., Swietlicki, E., Tonev, D., Vaughan, G., Zdimal, V., Baltensperger, U., Doussin, J.-F., Kulmala, M., Pappalardo, G., Sorvari Sundet, S., and Vana, M.: Aerosol, Clouds and Trace Gases Research Infrastructure (ACTRIS): The European Research Infrastructure Supporting Atmospheric Science, Bulletin of the American Meteorological Society, 105, E1098–E1136, https://doi.org/10.1175/BAMS-D-23-0064.1, 2024.

Landgrebe, R.: Convergence with EU Air Protection Policies: Short Guide for ENP Partners and Russia, European Communities, https://www.ecologic.eu/sites/default/files/publication/2024/air_en.pdf, 2008.

Lasota, E., Houben, T., Polz, J., Schmidt, L., Glawion, L., Schäfer, D., Bumberger, J., and Chwala, C.: Interpretable Quality Control of Sparsely Distributed Environmental Sensor Networks Using Graph Neural Networks, Artificial Intelligence for the Earth Systems, 4, e240 032, https://doi.org/10.1175/AIES-D-24-0032.1, 2025.

Laurita, T., Mauceri, A., Cardellicchio, F., Lapenna, E., De Rosa, B., Trippetta, S., Mytilinaios, M., Amodio, D., Giunta, A., Ripepi, E., Colangelo, C., Papagiannopoulos, N., Morrongiello, F., Dema, C., Gagliardi, S., Cornacchia, C., Petracca Altieri, R. M., Amodeo, A., Rosoldi, M., Summa, D., Pappalardo, G., and Mona, L.: CIAO main upgrade: building up an ACTRIS-compliant aerosol in situ laboratory, Atmospheric Measurement Techniques, 18, 2373–2396, https://doi.org/10.5194/amt-18-2373-2025, 2025.

Li, X., Feng, M., Ran, Y., Su, Y., Liu, F., Huang, C., Shen, H., Xiao, Q., Su, J., Yuan, S., and Guo, H.: Big Data in Earth system science and progress towards a digital twin, Nature Reviews Earth & Environment, 4, 319–332, https://doi.org/10.1038/s43017-023-00409-w, 2023.

Loescher, H. W., Vargas, R., Mirtl, M., Morris, B., Pauw, J., Yu, X., Kutsch, W., Mabee, P., Tang, J., Ruddell, B. L., Pulsifer, P., Bäck, J., Zacharias, S., Grant, M., Feig, G., Zhang, L., Waldmann, C., and Genazzio, M. A.: Building a Global Ecosystem Research Infrastructure to Address Global Grand Challenges for Macrosystem Ecology, Earth's Future, 10, https://doi.org/10.1029/2020ef001696, 2022.

Mollenhauer, H., Kasner, M., Haase, P., Peterseil, J., Wohner, C., Frenzel, M., Mirtl, M., Schima, R., Bumberger, J., and Zacharias, S.: Long-term environmental monitoring infrastructures in Europe: observations, measurements, scales, and socio-ecological representativeness, Science of The Total Environment, 624, 968–978, https://doi.org/10.1016/j.scitotenv.2017.12.095, 2018.

Moosmüller, H., Chakrabarty, R. K., Ehlers, K. M., and Arnott, W. P.: Absorption Ångström coefficient, brown carbon, and aerosols: basic concepts, bulk matter, and spherical particles, Atmospheric Chemistry and Physics, 11, 1217–1225, https://doi.org/10.5194/acp-11-1217-2011, 2011.

https://doi.org/10.5194/egusphere-2026-235
Preprint. Discussion started: 13 March 2026

Mueller, T., Paixao, M., Pfeifer, S., and Wiedensohler, A.: Scattering Coefficients and Asymmetry Parameters derived from the Polar Nephelometer Aurora4000, Zenodo, https://doi.org/10.5281/ZENODO.5588445, 2012.

Müller, T. and Fiebig, M.: ACTRIS In Situ Aerosol: Guidelines for Manual QC of Ecotech Aurora 4000/3000 Integrating Nephelometer Data, Guidelines v0, https://www.actris-ecac.eu/files/2020-08-24_ACTRIS_Aurora_nephelometers_v0.pdf, 2020.

Müller, T. and Fiebig, M.: ACTRIS In Situ Aerosol: Guidelines for Manual QC of AE33 absorption photometer data, Guidelines v1, https://www.actris-ecac.eu/pluginAppObj/pluginAppObj_225_189/2021-09-14_ACTRIS_AE33_v1.pdf, 2021.

Müller, T., Henzing, J. S., de Leeuw, G., Wiedensohler, A., Alastuey, A., Angelov, H., Bizjak, M., Collaud Coen, M., Engström, J. E., Gruening, C., Hillamo, R., Hoffer, A., Imre, K., Ivanow, P., Jennings, G., Sun, J. Y., Kalivitis, N., Karlsson, H., Komppula, M., Laj, P., Li, S.-M., Lunder, C., Marinoni, A., Martins dos Santos, S., Moerman, M., Nowak, A., Ogren, J. A., Petzold, A., Pichon, J. M., Rodriquez, S., Sharma, S., Sheridan, P. J., Teinilä, K., Tuch, T., Viana, M., Virkkula, A., Weingartner, E., Wilhelm, R., and Wang, Y. Q.: Characterization and intercomparison of aerosol absorption photometers: result of two intercomparison workshops, Atmospheric Measurement Techniques, 4, 245–268, https://doi.org/10.5194/amt-4-245-2011, 2011.

Müller, T., Laborde, M., Kassell, G., and Wiedensohler, A.: Design and performance of a three-wavelength LED-based total scatter and backscatter integrating nephelometer, Atmospheric Measurement Techniques, 4, 1291–1303, https://doi.org/10.5194/amt-4-1291-2011, 2011.

Napoly, A., Grassmann, T., Meier, F., and Fenner, D.: Development and Application of a Statistically-Based Quality Control for Crowdsourced Air Temperature Data, Frontiers in Earth Science, 6, 118, https://doi.org/10.3389/feart.2018.00118, 2018.

NOAA Global Monitoring Laboratory: Using FORGE for Data Viewing and Editing, https://gml.noaa.gov/aero/docs/Using_FORGE.pdf, accessed 2026-03-11, 2022.

NOAA Global Monitoring Laboratory: Aerosol Group Software, https://gml.noaa.gov/aero/sw.html, accessed 2026-03-11, n.d.

Ohnemus, T., Dirnböck, T., Bäck, J., Gaube, V., Kühn, I., Mirtl, M., Mollenhauer, H., Vereecken, H., and Zacharias, S.: Fitness for future: eLTER RI's representation of climate and land use change, Ecological Indicators, 171, 113 159, https://doi.org/10.1016/j.ecolind.2025.113159, 2025.

Okorn, K. and Iraci, L. T.: An overview of outdoor low-cost gas-phase air quality sensor deployments: current efforts, trends, and limitations, Atmospheric Measurement Techniques, 17, 6425–6457, https://doi.org/10.5194/amt-17-6425-2024, 2024.

Ośródka, K., Otop, I., and Szturc, J.: Automatic quality control of telemetric rain gauge data providing quantitative quality information (RainGaugeQC), Atmospheric Measurement Techniques, 15, 5581–5597, https://doi.org/10.5194/amt-15-5581-2022, 2022.

Petzold, A., Ogren, J. A., Fiebig, M., Laj, P., Li, S.-M., Baltensperger, U., Holzer-Popp, T., Kinne, S., Pappalardo, G., Sugimoto, N., Wehrli, C., Wiedensohler, A., and Zhang, X.-Y.: Recommendations for reporting "black carbon" measurements, Atmospheric Chemistry and Physics, 13, 8365–8379, https://doi.org/10.5194/acp-13-8365-2013, 2013.

Petzold, A., Thouret, V., Gerbig, C., Zahn, A., Brenninkmeijer, C. A. M., Gallagher, M., Hermann, M., Pontaud, M., Ziereis, H., Boulanger, D., Marshall, J., Nédélec, P., Smit, H. G. J., Friess, U., Flaud, J.-M., Wahner, A., Cammas, J.-P., Volz-Thomas, A., and Team, I.: Global-scale atmosphere monitoring by in-service aircraft – current achievements and future prospects of the European Research Infrastructure IAGOS, Tellus B: Chemical and Physical Meteorology, 67, 28 452, https://doi.org/10.3402/tellusb.v67.28452, 2015.

Petzold, A., Bundke, U., Hienola, A., Laj, P., Lund Myhre, C., Vermeulen, A., Adamaki, A., Kutsch, W., Thouret, V., Boulanger, D., Fiebig, M., Stocker, M., Zhao, Z., and Asmi, A.: Opinion: New directions in atmospheric research offered by research infrastructures combined with open and data-intensive science, Atmospheric Chemistry and Physics, 24, 5369–5388, https://doi.org/10.5194/acp-24-5369-2024, 2024.

Ran, L., Zhou, F., Deng, Z., Zhou, M., and Wang, P.: A method to obtain scattering phase function based on particle size distribution and refractive index retrieved from Aurora 4000 multi-angle scattering measurements: A numerical study, Atmospheric Environment, 315, 120 138, https://doi.org/10.1016/j.atmosenv.2023.120138, 2023.

Reichstein, M., Camps-Valls, G., Stevens, B., Jung, M., Denzler, J., Carvalhais, N., and Prabhat: Deep learning and process understanding for data-driven Earth system science, Nature, 566, 195–204, https://doi.org/10.1038/s41586-019-0912-1, 2019.

RI-URBANS: WP6 Deliverable D46 (D6.1): Guidance documents on measurements & modelling of novel air quality pollutants: Black carbon (BC) determinations, Tech. rep., https://riurbans.eu/wp-content/uploads/2024/11/ENV_GUIDANCE-DOCUMENT_ST2_BC_Definitive.pdf, 2024.

Savadkoohi, M., Pandolfi, M., Reche, C., Niemi, J. V., Mooibroek, D., Titos, G., Green, D. C., Tremper, A. H., Hueglin, C., Liakakou, E., Mihalopoulos, N., Stavroulas, I., Artiñano, B., Coz, E., Alados-Arboledas, L., Beddows, D., Riffault, V., De Brito, J. F., Bastian, S., Baudic, A., Colombi, C., Costabile, F., Chazeau, B., Marchand, N., Gómez-Amo, J. L., Estellés, V., Matos, V., van der Gaag, E., Gille, G., Luoma, K., Manninen, H. E., Norman, M., Silvergren, S., Petit, J.-E., Putaud, J.-P., Rattigan, O. V., Timonen, H., Tuch, T., Merkel, M., Weinhold, K., Vratolis, S., Vasilescu, J., Favez, O., Harrison, R. M., Laj, P., Wiedensohler, A., Hopke, P. K., Petäjä, T., Alastuey, A., and Querol, X.: The variability of mass concentrations and source apportionment analysis of equivalent black carbon across urban Europe, Environment International, 178, 108 081, https://doi.org/10.1016/j.envint.2023.108081, 2023.

Savadkoohi, M., Pandolfi, M., Favez, O., Putaud, J.-P., Eleftheriadis, K., Fiebig, M., Hopke, P. K., Laj, P., Wiedensohler, A., Alados-Arboledas, L., Bastian, S., Chazeau, B., Álvaro Clemente María, Colombi, C., Costabile, F., Green, D. C., Hueglin, C., Liakakou, E., Luoma, K., Listrani, S., Mihalopoulos, N., Marchand, N., Močnik, G., Niemi, J. V., Ondráček, J., Petit, J.-E., Rattigan, O. V., Reche, C., Timonen, H., Titos, G., Tremper, A. H., Vratolis, S., Vodička, P., Funes, E. Y., Zíková, N., Harrison, R. M., Petäjä, T., Alastuey, A., and Querol, X.: Recommendations for reporting equivalent black carbon (eBC) mass concentrations based on long-term pan-European in-situ observations, Environment International, 185, 108 553, https://doi.org/10.1016/j.envint.2024.108553, 2024.

https://doi.org/10.5194/egusphere-2026-235
Preprint. Discussion started: 13 March 2026

Schäfer, D., Palm, B., Lünenschloß, P., Schmidt, L., and Bumberger, J.: Reproducible quality control of time series data with SaQC, in: EGU General Assembly 2023, Vienna, Austria, https://doi.org/10.5194/egusphere-egu23-12971, eGU23-12971, 2023.

Schmidt, L., Schäfer, D., Geller, J., Lünenschloss, P., Palm, B., Rinke, K., Rebmann, C., Rode, M., and Bumberger, J.: System for automated Quality Control (SaQC) to enable traceable and reproducible data streams in environmental science, Environmental Modelling & Software, 169, 105 809, https://doi.org/10.1016/j.envsoft.2023.105809, 2023.

Scully-Allison, C., Le, V., Fritzinger, E., Strachan, S., Harris, F. C., and Dascalu, S. M.: Near Real-time Autonomous Quality Control for Streaming Environmental Sensor Data, Procedia Computer Science, 126, 1656–1665, https://doi.org/10.1016/j.procs.2018.08.139, 2018.

Sheldon, W. M. J.: Dynamic, Rule-based Quality Control Framework for Real-time Sensor Data, in: Proceedings of the Environmental Information Management 2008 Conference (EIM 2008), https://gce-lter.marsci.uga.edu/public/files/pubs/wsheldon_dynamic_qc_eimc2008_final.pdf, 2008.

Suchánková, L., Mbengue, S., Zíková, N., Šmejkalová, A. H., Prokeš, R., Holoubek, I., and Ždímal, V.: A seven-year-based characterization of aerosol light scattering properties at a rural central European site, Atmospheric Environment, 319, 120 292, https://doi.org/10.1016/j.atmosenv.2023.120292, 2024.

Taylor, J. R. and Loescher, H. L.: Automated quality control methods for sensor data: a novel observatory approach, Biogeosciences, 10, 4957–4971, https://doi.org/10.5194/bg-10-4957-2013, 2013.

Teri, M., Müller, T., Gasteiger, J., Valentini, S., Horvath, H., Vecchi, R., Bauer, P., Walser, A., and Weinzierl, B.: Impact of particle size, refractive index, and shape on the determination of the particle scattering coefficient – an optical closure study evaluating different nephelometer angular truncation and illumination corrections, Atmospheric Measurement Techniques, 15, 3161–3187, https://doi.org/10.5194/amt-15-3161-2022, 2022.

U.S. Environmental Protection Agency: Ambient Air Monitoring Quality Assurance, https://www.epa.gov/amtic/ambient-air-monitoring-quality-assurance, Accessed: 2026-01-02, 2026.

Valenzuela, A., Olmo, F., Lyamani, H., Antón, M., Titos, G., Cazorla, A., and Alados-Arboledas, L.: Aerosol scattering and absorption Angström exponents as indicators of dust and dust-free days over Granada (Spain), Atmospheric Research, 154, 1–13, https://doi.org/10.1016/j.atmosres.2014.10.015, 2015.

World Meteorological Organization: An Update on Low-cost Sensors for the Measurement of Atmospheric Composition, WMO Report 1215, World Meteorological Organization (WMO), World Health Organization (WHO), International Global Atmospheric Chemistry project (IGAC), Co-operative Programme for Monitoring and Evaluation of the Long-range Transmission of Air Pollutants in Europe (EMEP), United Nations Environment Programme (UNEP), ISBN 978-92-63-11215-6, https://library.wmo.int/idurl/4/37465, 2021.

World Meteorological Organization (WMO): WMO/GAW Aerosol Measurement Procedures, Guidelines and Recommendations, Tech. rep., https://doi.org/10.5281/zenodo.11145571, 2016.

World Meteorological Organization (WMO); United Nations Environment Programme (UNEP); International Global Atmospheric Chemistry project (IGAC): Integrating Low-cost Sensor Systems and Networks to Enhance Air Quality Applications, GAW Report 293, https://library.wmo.int/records/item/68924-integrating-low-cost-sensor-systems-and-networks-to-enhance-air-quality-applications, 2024.

Wu, H., Tang, X., Wang, Z., Wu, L., Lu, M., Wei, L., and Zhu, J.: Probabilistic Automatic Outlier Detection for Surface Air Quality Measurements from the China National Environmental Monitoring Network, Advances in Atmospheric Sciences, 35, 1522–1532, https://doi.org/10.1007/s00376-018-8067-9, 2018.

Yus-Díez, J., Bernardoni, V., Močnik, G., Alastuey, A., Ciniglia, D., Ivančič, M., Querol, X., Perez, N., Reche, C., Rigler, M., Vecchi, R., Valentini, S., and Pandolfi, M.: Determination of the multiple-scattering correction factor and its cross-sensitivity to scattering and wavelength dependence for different AE33 Aethalometer filter tapes: a multi-instrumental approach, Atmospheric Measurement Techniques, 14, 6335–6355, https://doi.org/10.5194/amt-14-6335-2021, 2021.

Zacharias, S., Loescher, H. W., Bogena, H., Kiese, R., Schrön, M., Attinger, S., Blume, T., Borchardt, D., Borg, E., Bumberger, J., Chwala, C., Dietrich, P., Fersch, B., Frenzel, M., Gaillardet, J., Groh, J., Hajnsek, I., Itzerott, S., Kunkel, R., Kunstmann, H., Kunz, M., Liebner, S., Mirtl, M., Montzka, C., Musolff, A., Pütz, T., Rebmann, C., Rinke, K., Rode, M., Sachs, T., Samaniego, L., Schmid, H. P., Vogel, H.-J., Weber, U., Wollschläger, U., and Vereecken, H.: Fifteen Years of Integrated Terrestrial Environmental Observatories (TERENO) in Germany: Functions, Services, and Lessons Learned, Earth's Future, 12, e2024EF004 510, https://doi.org/10.1029/2024EF004510, e2024EF004510 2024EF004510, 2024.

Zhao, W., Tan, W., Zhao, G., Shen, C., Yu, Y., and Zhao, C.: Determination of equivalent black carbon mass concentration from aerosol light absorption using variable mass absorption cross section, Atmospheric Measurement Techniques, 14, 1319–1331, https://doi.org/10.5194/amt-14-1319-2021, 2021.

Zheng, H., Kong, S., Ding, D., Savadkoohi, M., Song, C., Zheng, M., and Harrison, R. M.: Black carbon aerosols in China: spatial-temporal variations and lessons from long-term atmospheric observations, Atmospheric Chemistry and Physics, 25, 16 363–16 386, https://doi.org/10.5194/acp-25-16363-2025, 2025.

Zibordi, G., D'Alimonte, D., and Kajiyama, T.: Automated Quality Control of AERONET-OC LWN Data, Journal of Atmospheric and Oceanic Technology, 39, 1961 – 1972, https://doi.org/10.1175/JTECH-D-22-0029.1, 2022.

https://doi.org/10.5194/egusphere-2026-235
Preprint. Discussion started: 13 March 2026

Table 1. Table listing selected time ranges where certain instrument anomalies were identified. Each anomaly comprises data for both instruments, even though the anomalies appeared only for one of them.

ID	Description Short	Description	Instrument	Site	Start Time	End Time
bc1	drop and constants	constant drop in data	Aethalometer	TROPOS	2022-09-29 00:00:00	2022-10-01 00:00:00
bc2	drop and constants 2	extended constant drop in data	Aethalometer	TROPOS	2022-10-01 00:00:00	2022-10-04 00:00:00
bc3	outliers	outliers in measurements	Aethalometer	TROPOS	2022-10-07 00:00:00	2022-10-08 00:00:00
bc4	outliers	extended outliers in data	Aethalometer	TROPOS	2024-01-10 00:00:00	2024-01-20 00:00:00
bc5	noise	high noise levels	Aethalometer	TROPOS	2024-01-10 00:00:00	2024-01-29 00:00:00
bc6	rh inlet	anomaly in `rh_inlet` readings	Aethalometer	TROPOS	2024-01-10 00:00:00	2024-02-26 00:00:00
bc7	noise	noise at the beginning, then normal signal	Aethalometer	TROPOS	2024-01-01 00:00:00	2024-01-30 00:00:00
ls1	long period	long period signal with multiple anomalies	Nephelometer	TROPOS	2024-01-17 00:00:00	2024-03-01 00:00:00
ls3	drop and constants	short constant flag period	Nephelometer	TROPOS	2022-05-25 00:00:00	2022-05-26 00:00:00
ls4	range	short range flag	Nephelometer	TROPOS	2022-05-25 00:00:00	2022-05-26 00:00:00
ls5	drops, outliers	outlier period	Nephelometer	TROPOS	2024-02-25 00:00:00	2024-02-29 00:00:00
bc1-mel	constant	constants	Aethalometer	Melpitz	2024-11-30 00:00:00	2024-12-02 00:00:00
bc2-mel	peaks	some reasonable peaks in that time range	Aethalometer	Melpitz	2024-11-09 16:00:00	2024-11-10 01:00:00
bc3-mel	noise	parts with higher and parts with lower noise	Aethalometer	Melpitz	2024-11-20 00:00:00	2024-11-23 00:00:00
bc4-mel	peaks	peaks with some unreasonable low areas	Aethalometer	Melpitz	2024-11-30 06:00:00	2024-12-02 18:00:00
bc5-mel	peaks	high peaks with high background	Aethalometer	Melpitz	2024-12-27 12:00:00	2024-12-30 12:00:00
ls1-mel	peaks-flats	peaks with flats and constants	Nephelometer	Melpitz	2024-11-09 14:00:00	2024-11-10 04:00:00
ls2-mel	outlier	a single outlier surrounded by little background noise and increasing noise after it	Nephelometer	Melpitz	2024-11-29 00:00:00	2024-11-30 00:00:00
ls3-mel	outlier-and-flats	high outlier with flats a few hours earlier and later	Nephelometer	Melpitz	2024-12-04 00:00:00	2024-12-06 00:00:00
ls4-mel	signal-and-flats	a reasonable signal and some flats once each day after	Nephelometer	Melpitz	2024-12-17 00:00:00	2024-12-20 12:00:00
ls5-mel	system-start	system start up with different states following normal operation	Nephelometer	Melpitz	2025-01-30 14:00:00	2025-01-30 16:00:00
ls6-mel	peaks	some reasonable peaks and flats after	Nephelometer	Melpitz	2025-02-16 12:00:00	2025-02-17 04:00:00
ls7-mel	outlier-and-signal	a very high outlier followed by a single a few days later	Nephelometer	Melpitz	2025-03-05 00:00:00	2025-03-13 00:00:00
ls8-mel	system-failure-to-outlier	system was down then an outlier appeared after back to operation	Nephelometer	Melpitz	2025-04-14 00:00:00	2025-04-14 21:00:00

https://doi.org/10.5194/egusphere-2026-235
Preprint. Discussion started: 13 March 2026

Table 2. Overview of selected anomalies for both measurement sites and instruments. For each case, the number of data points, required QC time and resulting flags are listed.

ID	Site	Aethalometer (AE33)					Nephelometer (Aurora 4000)				
		No. data points	QC time [s]	BAD	DOUBT	GOOD	No. data points	QC time [s]	BAD	DOUBT	GOOD
bc1	TROPOS	2 279	33	423	43	1 813	13 058	9	257	61	12 740
bc2	TROPOS	4 336	39	148	53	4 135	25 815	11	471	90	25 254
bc3	TROPOS	1 458	33	167	16	1 275	8 603	7	127	30	8 446
bc4	TROPOS	12 213	47	742	11 103	368	21 238	11	832	77	20 329
bc5	TROPOS	24 430	75	1 415	11 185	11 830	93 830	24	3 410	302	90 118
bc6	TROPOS	99 998	591	4 171	12 721	83 106	327 059	253	11 276	1 140	314 643
bc7	TROPOS	25 680	257	1 501	11 200	12 979	101 764	94	3 652	332	97 780
ls1	TROPOS	101 797	187	4 621	8 822	88 354	361 364	78	12 339	1 260	347 765
ls3	TROPOS	734	29	1	0	733	8 531	8	250	30	8 251
ls4	TROPOS	734	29	1	0	733	8 531	8	250	30	8 251
ls5	TROPOS	5 809	43	380	54	5 375	34 357	13	1 171	120	33 066
bc1-mel	Melpitz	17 273	109	17 273	0	0	17 265	32	230	60	16 975
bc2-mel	Melpitz	3 239	93	511	84	2 644	3 236	22	116	177	2 943
bc3-mel	Melpitz	25 889	120	25 134	0	755	25 892	38	344	90	25 458
bc4-mel	Melpitz	21 581	114	21 581	0	0	21 574	35	230	60	21 284
bc5-mel	Melpitz	25 893	122	3 453	567	21 873	25 906	38	348	90	25 468
ls1-mel	Melpitz	5 036	94	866	136	4 034	5 033	23	116	177	4 740
ls2-mel	Melpitz	8 638	103	8 638	0	0	8 632	25	115	30	8 487
ls3-mel	Melpitz	17 263	118	17 263	0	0	17 262	31	348	90	16 824
ls4-mel	Melpitz	30 206	136	4 092	1 310	24 804	30 209	44	503	126	29 580
ls5-mel	Melpitz	531	87	82	30	419	701	19	277	11	413
ls6-mel	Melpitz	5 753	31	408	76	5 269	5 753	7	115	30	5 608
ls7-mel	Melpitz	68 133	59	7 742	1 356	59 035	68 920	20	1 045	247	67 628
ls8-mel	Melpitz	3 061	28	1 039	79	1 943	3 845	6	187	26	3 632

https://doi.org/10.5194/egusphere-2026-235
Preprint. Discussion started: 13 March 2026

Table A1. Table of configured SaQC tests and their parameterization for the AE33 Aethalometers data.

Variable	SaQC Test	Label and Configuration	Flag
DEVICE CONTROL VARIABLES			
flow_1	flagRange	BAD:flagRange: flow_1 $<$ 3.7 or flow_1 $>$ 4.05	BAD
flow_2	flagRange	BAD:flagRange: flow_2 $<$ 0.8 or 1.3 $<$ flow_2	BAD
flow_c	flagRange	BAD:flagRange: flow_c $<$ 4.8 or flow_c $>$ 5	BAD
	flagByScatterLowpass	ebc_w1: window=50 min, sub_window=4 min, thresh=0.11843143248405742, sub_thresh=0.06125258741743177	DOUBTFUL
status_inst	flagGeneric	BAD:flagGeneric: status_inst $\neq$ 0	BAD
rh_inlet	flagRange	BAD:flagRange: rh_inlet $<$ 0 or rh_inlet $>$ 50	BAD
	flagRange	DOUBT:flagRange: 40 $<$ rh_inlet $<$ 50	DOUBTFUL
status_valve	flagGeneric	BAD:flagGeneric: status_valve $\neq$ 0	BAD
	propagateFlags	DOUBT:flagPropagate: status_valve bfill 5 min	DOUBTFUL
	propagateFlags	BAD:flagPropagate: status_valve ffill 10 min	BAD
status_ctrl	flagGeneric	BAD:flagGeneric: status_ctrl $\neq$ 0	BAD
status_det	flagGeneric	BAD:flagGeneric: status_det $\neq$ 0 and not 10	BAD
status_led	flagGeneric	BAD:flagGeneric: status_led $\neq$ 0 and not 10	BAD
numflag	flagGeneric	BAD:flagGeneric: numflag $\neq$ 0	BAD
CHANNEL SPECIFIC VARIABLES			
ebc_wx	flagByScatterLowpass	DOUBT:optimized flagByScatterLowpass: ebc	DOUBTFUL
	flagConstants	BAD:flagConstants: thresh=0.012, window=12 min of {target}	BAD
	flagRange	BAD:Range: {target} $<$ -0.075 or {target} $>$ 100	BAD
	flagRange	DOUBT:Range: {target} $<$ 0.05 or {target} $>$ 50	DOUBTFUL
	andGroup	BAD:downward-spikes	BAD
	– flagUniLOF	thresh=1.1, n=400	
	– flagGeneric	λx: $x < x$.rolling("1H").mean()	
attn_wx_sp1	flagRange	BAD:flagRange: {attn_wx_sp1} $<$ 0 or {attn_wx_sp1} $>$ 120	BAD
	flagRange	DOUBT:flagRange: 80 $<$ {attn_wx_sp1} $<$ 120	DOUBTFUL
DERIVED VARIABLES			
AAE	flagRange	DOUBT:{aae} $<$ 0.6 or {aae} $>$ 2.5	DOUBTFUL
(UVG, GR, UVR)	flagRange	BAD:{aae} $<$ 0.5 or {aae} $>$ 3.0	BAD
	flagGeneric	BAD:Discrepancy: UVR + 0.7 $<$ UVG or UVR - 0.7 $>$ GR	BAD

https://doi.org/10.5194/egusphere-2026-235
Preprint. Discussion started: 13 March 2026

Table A2. Table of configured SaQC tests and their parameterization for the Aurora 4000 Nephelometer data.

Variable	SaQC Test	Label and Configuration	Flag
DEVICE CONTROL VARIABLES			
rh_int	flagRange	BAD:flagRange: rh_int $<$ 0 or rh_int $>$ 50	BAD
	flagRange	DOUBT:flagRange: 40 $<$ rh_int $<$ 50	DOUBTFUL
state_dio	flagGeneric	BAD:flagGeneric: state_dio $\neq$ 0 and not 7	BAD
state_major	flagGeneric	BAD:flagGeneric: state_major $\neq$ 0	BAD
		DOUBT:flagPropagate: state_major bfill 5 min	DOUBTFUL
		BAD:flagPropagate: state_major ffill 20 min	BAD
pres_int	flagRange	BAD:flagRange: pres_int $<$ 950 or pres_int $>$ 1030	BAD
temp_int	flagRange	BAD:flagRange: 233.15 $<$ temp_int $<$ 313.15	BAD
CHANNEL SPECIFIC VARIABLES			
sca (450, 525, 635)	flagConstants	BAD:flagConstants: thresh=0.012, window=12 min of {target}	BAD
	flagRange	BAD:flagRange: {targets} $<$ 0 or {targets} $>$ 20000	BAD
	flagRange	DOUBT:flagRange: 0.05 $<$ {targets} $<$ 6000	DOUBTFUL
	flagByScatterLowpass	sca450: window=22 min, sub_window=5 min, thresh=25.735605807619283, sub_thresh=20.09818377471357	DOUBTFUL
DERIVED VARIABLES			
SAE (BG, GR, BR)	flagRange	BAD:{sae} $<$ 0 or {sae} $>$ 3.5	BAD
	flagGeneric	BAD:Discrepancy: BR + 1.0 $<$ BG or BR - 1.0 $>$ GR	BAD